IEEE Access
Multidisciplinary | Rapid Review | Open Access Journal

Received July 22, 2020, accepted August 3, 2020, date of publication August 10, 2020, date of current version August 21, 2020.

Digital Object Identifier 10.1109/ACCESS.2020.3015243

Short-Term Predictive Power Management of PV-Powered Nanogrids

SANGKEUM LEE[1], HOJUN JIN[1], LUIZ FELIPE VECCHIETTI[1], JUNHEE HONG[2], (Member, IEEE), AND DONGSOO HAR[1], (Senior Member, IEEE)

[1]The Cho Chun Shik Graduate School of Green Transportation, Korea Advanced Institute of Science and Technology, Daejeon 34141, South Korea
[2]Department of Energy IT, Gachon University, Seongnam 13120, South Korea

Corresponding author: Dongsoo Har (dshar@kaist.ac.kr)

This work was supported by the Energy Cloud Research and Development Program through the National Research Foundation of Korea (NRF) funded by the Ministry of Science, ICT, under Grant 2019M3F2A1073314.

ABSTRACT Optimization of power management of nanogrid based on short-term prediction of PV power production and consequent EV charging/discharging is proposed. Goal of power management is to reduce time-based electricity cost and total delay. To achieve the goal, efficiency in the combined use of PV power and EV charging/discharging power is important. Unlike the PV power used ahead of costly grid power and entirely dependent on weather condition, timing of EV charging/discharging depends on power management scheme. In order to find out the timing for EV charging/discharging, short-term prediction of PV power production is considered as a key contributor. When PV power production is predicted to decrease in short-term, e.g., 10minutes, discharging power of EVs can compensate the loss and, when predicted to increase in short-term, EVs are charged to capitalize on the gain. Short-term prediction of PV power production is performed by long short-term memory (LSTM) network trained and validated by dataset of PV power production over 1 year. In addition, variation of outdoor temperature in relation to indoor temperature is factored in to determine the timing for EV charging/discharging. Our work is comprehensive in that various electric appliances as well as PV source and EVs are taken into account for power management of nanogrid. Simulation results show the cost benefit obtained from the short-term prediction of PV power production and consequent EV charging/discharging while managing peak demand below maximum allowed level.

INDEX TERMS Power management, nanogrid, peak load shifting, PV power, LSTM network.

I. INTRODUCTION

Recently, nanogrids gain growing popularity due to their flexibility in design, implementation, and control. Nanogrids with various electric appliances can be defined as kW scale smart grids that can combine different power sources with the help of IT technology. They often use expandable DC power sources for possible reconfiguration of electric vehicles (EVs), energy storage system (ESS), and electric appliances. Typical DC power source for the operation of nanogrids is photovoltaic (PV) panels [1]. To control the power consumption of various electric loads, peak-shaving, peak load shifting, and other management techniques are utilized. With the presence of various electric loads and mixed power source, grid and PV panels, it is difficult to achieve power balancing between demand and supply. To achieve power balancing requires efficient power allocation over electric loads, which represents the optimal matching of demand to supply from the viewpoint of electricity cost [2]. Topologies of nanogrids with distributed power sources enable ancillary services such as voltage support by reactive power injection, fault recovery aids supported by devices with built-in intelligence, reduction of power losses, and enhancement of local network power quality [3]. In order to improve the reliability and resilience, distributed nanogrids can be integrated with grid-forming energy storage [4]. The distributed and decentralized nanogrids can resolve more directly and more efficiently the issue of power balancing between local power demand and local power supply. As a result, the costs of utilities for building grid infrastructure that can provide low cost electricity are reduced [5], [6]. Therefore, distributed nanogrids can be beneficial for consumers and utilities.

The electric loads in a nanogrid include electric appliances, ESS, and EVs. Optimal power management in response to the demand of these electric loads is presented in [7].

The associate editor coordinating the review of this manuscript and approving it for publication was Alexander Micallef.

In DC nanogrids, the electric loads are DC type and electric appliances can be classified into shiftable and non-shiftable ones. In case of shiftable appliances, scheduling is allowed when the instantaneous power consumption of the nanogrid is excessively high. Of these electric appliances, heater, ventilation fan, and air-conditioner (HVAC) operate to control temperature, humidity, and CO_2 quality of the household. Operation of HVAC with renewable sources for securing living comfort has been investigated in the literature [8]. The heater and air-conditioner consume relatively high power as compared to other electric appliances. Because of the high power consumption of HVAC, other high power electric appliances might not be used simultaneously with HVAC even though those are non-shiftable appliances [9]. The change of the instantaneous power consumption of electrical appliances located in a nanogrid is basically determined by the behavior of residents, which can be modeled by the data on probabilistic use of electric appliances [10] in conjunction with resident location [11], [12].

The adoption of EVs is being encouraged due to environmental issues. The EVs have a substantial impact on the operation and scheduling of electric appliances when integrated into the nanogrid as a new type of load [13]. On the other hand, the batteries of the EVs can be utilized as ESSs delivering power to nanogrids at peak hours of load demand. The vehicle-to-grid (V2G) technology, which implements bidirectional power flow between EVs and grid, can be applied for efficient nanogrid power management. The V2G configuration can be adopted to increase the performance of nanogrids measured in terms of reliability, stability, efficiency, and economic feasibility [14]–[18]. In addition, the EV as an ESS enables the grid to optimize the use of renewable energy which is inherently intermittent and unpredictable [19]. The dynamic EV charging can thus increase economic efficiency and make higher use of renewable energy for nanogrid operation [20]. The vehicle-to-home (V2H) technology, which is a subordinate concept of V2G, represents that the EV is connected to a home grid for charging and discharging by onboard or offboard bidirectional charger [21].

Enrollment of EVs is being incentivized as an important measure to reduce the CO_2 emission and air pollution in many countries such as Korea [22]. To perform power management in conjunction with EVs, modeling of EV charging and discharging is required. In [23]–[25], the Markov chain is used to capture and simulate the vehicle use pattern. In [26], an EV charging model with a Markov chain is based on the time-of-use rate and state of charging (SOC) curve. Optimization of EV charging and discharging based on electricity cost is described in [27] with a V2G configuration. Due to the relatively high charging/discharging power of an EV, its charging pattern may affect significantly the overall electric load profile of nanogrid. Therefore, it is important to develop the EV charging/discharging model accounting for stochastic car travel behaviors and charging needs. PV power production in conjunction with EV charging/discharging is considered as an effective way to accommodate eco-friendly power management [28]. Similar to the use of PV power for various applications [29]–[31], PV-assisted charging station for EVs have been studied [32], [33]. To ensure efficient use of PV power, prediction of PV power production is helpful, since predictive power management can take future operating condition(s) into account for improved results.

To this end, artificial neural networks such as long short-term memory (LSTM) [34] network can be adopted. The LSTM network has been used for various applications [35], [36]. According to the forecasting horizon, the forecasting model can be categorized into three categories: short-term forecasts upto one week, medium-term forecasts from one week to one year, and long-term forecasts over one year. In this work, the short-term forecast of PV power production is considered for nanogrid power management. However, the methodology making use of the LSTM network remains valid even when the mid-term or long-term forecast is used for power management. Similar to the forecasting of PV power production, forecasting of EV charging demand is investigated by big data technology [37].

The demand response (DR) program can be described as an incentive to make lower use of electricity when the market rate of electricity or demand for electricity is high [38]. In response to the DR, shiftable electric appliances can be scheduled within the maximum allowed delay. Likewise, scheduling of EV charging is made, following the DR program [39], [40]. Optimal scheduling of EV charging to fill the valleys in the electric load profile is investigated in [41]. The DR strategy with a bi-directional energy exchange between EV and ESS in V2G configuration is investigated in [40], [42], [43]. Optimized power management is considered in this paper as the optimization process leading to the lowest electricity cost as well as the minimum delay of the scheduling of shiftable appliances [44]. For such multi-objective optimization, the genetic algorithm (GA) [45], [46] can be used. In general, the objectives of optimization for home energy management can be load profile optimization, cost minimization, revenue maximization, loss minimization, and system reliability optimization [47].

In this paper, predictive power management for nanogrids with the PV power source to reduce the electricity cost is presented. The proposed scheme can be divided into two stages: prediction and scheduling. In the prediction stage, the PV output is forecasted using a time series model learned by the LSTM network. In the scheduling stage, the EV charging/discharging and scheduling of shiftable electric appliances are determined based on the result of the first stage. The LSTM network predicts PV power production over time to coordinate EV charging/discharging and operations of other electric appliances in a way that total electricity cost and total delay of scheduling are to be simultaneously minimized. Due to PV power used as a primary power resource and high charging/discharging power of each EV, the main concern of power management is the interrelation between PV power and EV charging/discharging.

The main contributions of this paper are as follows.

- Multi-objective optimization to minimize electricity cost and total delay simultaneously is presented for power management of nanogrid with PV source and EV as secondary power sources. Short-term prediction of PV power production and consequent EV charging/discharging are proposed for operation of PV source and EV.
- Cost-effective method for EV charging/discharging is proposed. EV charging/discharging to reduce electricity cost is dependent on trend of PV power production and temporal HVAC operation, as well as level of total power consumption. Therefore, EV charging/discharging conditions consist of policy-based condition involving PV power production and emergency-based condition associated with total power consumption.
- Optimization framework fit to power management of nanogrid with PV source and EV is presented. Within the framework, EV discharging based on short-term PV power production occurs at the time zone associated with significantly reduced electricity cost and total delay.
- Comprehensive work involving various electric appliances, including HVAC, provides methodology of the predictive power management for nanogrid with PV panels in V2H configuration.

Entire power source consists of grid power, PV power, and EV discharging power. Goal of power management of nanogrid is to reduce daily electricity cost quantified by DR program and total delay. Daily electricity cost is charged only to grid power. Therefore, it is important to reduce total amount of grid electricity consumed over a day and consume grid power in a cost-effective way. For this purpose, multi-objective optimization for power management of nanogrid is presented, taking EV charging/discharging depending on short-term prediction of PV power production and instantaneous HVAC operation into consideration.

Since PV power and EV discharging power can be used as secondary power sources, timely use of them is very important for reduction of electricity cost and total delay. While PV power production entirely depends on weather condition, timing for charging/discharging of EV can be controlled. Another important aspect of EV is that it has to be charged before discharging as secondary power source. When being charged, the EV is another electric appliance consuming electric power provided by grid or PV source. When being discharged, the EV can help reduce total power consumption. Therefore, timing for charging/discharging of EV should be controlled in a way that i) peak power consumption can be reduced below maximum allowed level and ii) daily electricity cost is decreased as compared to conventional charging/discharging solely based on the consideration of peak power consumption.

Based on typical pattern of PV power production and outdoor temperature variation over a day, downhill trend of PV power production is matched with the time zone around peak outdoor temperature causing large power consumption of HVAC. Operation of HVAC takes large portion of total power consumption. Therefore, rate of electricity is high over the time zone around peak outdoor temperature. As an alternative secondary source, discharged power of EV over the time zone can compensate the loss of PV power in downhill trend of PV power production and achieve reduction of electricity cost. However, exact time of peak PV power production right before the downhill trend is hard to estimate and there are local minima and maxima causing erroneous decision on trend. From this reason, more practical condition for EV discharging is the relation of PV power production $PW^{PV}_{LSTM}(n+1)$ predicted in short-term by LSTM network to current PV power production $PW^{PV}(n)$. When the PV power production is in downhill trend, i.e. $PW^{PV}(n) > PW^{PV}_{LSTM}(n+1)$ in most of time, permitting $PW^{PV}(n) < PW^{PV}_{LSTM}(n+1)$ occasionally, EV can compensate the loss. On the other hand, when the PV power production is in uphill trend, i.e. $PW^{PV}(n) < PW^{PV}_{LSTM}(n+1)$ in most of time, allowing $PW^{PV}(n) > PW^{PV}_{LSTM}(n+1)$ occasionally, EV is charged to capitalize on the gain. Considering rate of electricity and accumulated total delay in peak hours, EV discharging together with PV power in peak hours should be beneficial for optimal power management.

With EV being charged, grid power and PV power are consumed for electric appliances including EV and scheduling of shiftable electric appliances and EV charging becomes important for cost-efficient power management. On the other hand, when EV being discharged, grid power, PV power, and EV discharging power are consumed for electric appliances and scheduling of shiftable electric appliances is important for cost-efficient power management. Operation of HVAC depends on control mode specified by resident location and target temperature and use of specific shiftable and non-shiftable appliances is determined by resident behavior characterized by Markov chain model.

This paper is organized as follows. In Section II, the Markov chain model for resident behavior and random initiation of EV charging described by charging probability are explained. Section III provides details of the short-term predictive power management based on the LSTM network. Section IV presents simulation results obtained with four different settings of nanogrid operation and Section V concludes this paper.

II. MODELING OF NANOGRID OPERATION

The Jeju island in Korea initiated its project for the carbon-free island by 2030 with the main focus on the deployment of large-scale smart grids as shown in Fig.1(a) [22]. The project for carbon-free island aims at the development of business models by making use of smart grids employing renewable sources like PV panels and wind turbines. The smart grids use advanced metering infrastructure, ESS, energy management system for residences and offices. The operational concept of smart grids in Jeju island based on renewable energies can be adopted for nanogrids. Figure 1(b) shows the configuration of a grid-connected nanogrid consisting of 3 houses.

Peak rooftop of each house is covered with PV panels and each house is taken as a sub-nanogrid. An ESS denoted as "Battery" in Fig.1(b) is installed for the nanogrid to mitigate the intermittency of PV power production. Power conditioning systems such as DC/DC converters and PV panel inverters are to provide quality controlled DC power to electric appliances. Individual operations of electric appliances are controlled by the controller and instantaneous power consumption of each electric appliance is monitored by the smart meter and reported to the controller.

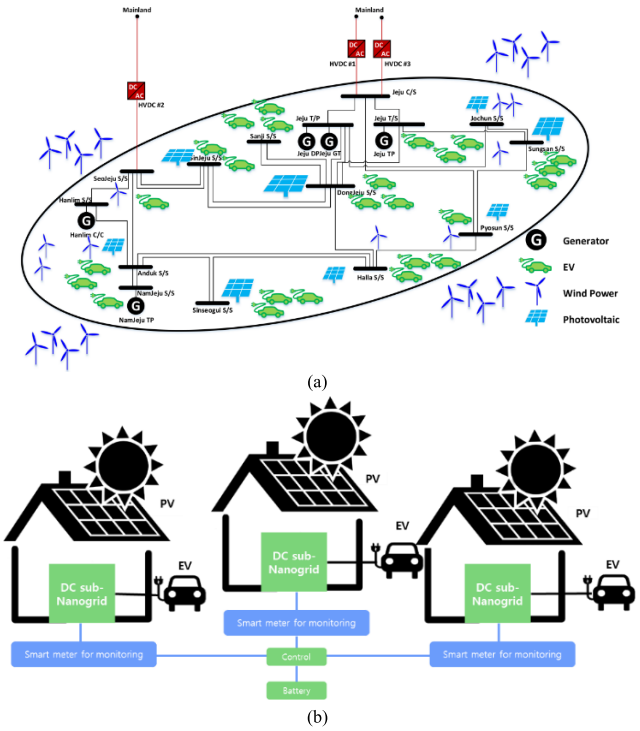

FIGURE 1. PV power production: (a) smart grids operated by PV power and wind power; (b) nanogrid employing PV panels [9]. The battery in (b) represents an ESS and can be replaced with the batteries of EVs.

In this work, nanogrids similar to the one in Fig. 1(b) are used. The nanogrid consists of houses equipped with PV panels for PV power production. Each house has 4 rooms where the shiftable and non-shiftable electric appliances are installed and connected to an EV charging/discharging system to form a V2G/V2H configuration. The nanogrid controller can communicate with electric appliances, EVs, and PV panels for power management. The resident behavior is stochastic in that he/she randomly transits between adjacent rooms and probabilistically uses an electric appliance in the room, where he/she locates, over every ten minutes. The HVAC determining the level of living comfort in each room can be activated in a controlled scenario.

The Markov chain model used for the modeling of resident's behavior regarding location and use of specific electric appliances is presented in Fig.3(a-c). The probability of a transition from the previous state to the current state depends only on the previous state as following

$$t_{ij} = \text{Prob}(o_t = v_j | o_{t-1} = v_i),$$
$$i, j = 1, 2, 3, 4 \; t_{ij} > 0 \; and \; \sum_{j=1}^{4} t_{ij} = 1 \quad (1)$$

where t_{ij} is the transition probability from state v_i to state v_j. Here, each state corresponds to a room and transition between adjacent rooms occurs at the beginning of every 10 minute time interval. When $i = j$, the resident stays in the same room over another 10 minutes. Figure 3(a) shows the floor plan of each house of the nanogrid. The R1, R2, R3, R4 indicate room numbers and only the room with the number R1 has paths to all other rooms. The resident probabilistically chooses an electric appliance immediately after transition and uses it over 10 minutes. There exist 9 shiftable and non-shiftable electric appliances, other than HVAC, installed in individual rooms with their specific power ratings: TV(non-shiftable)/130W and iron(shiftable)/1.23kW in R1, washing machine(shiftable)/242W and hair dryer(shiftable)/1kW in R2, audio(shiftable)/50W and computer(non-shiftable)/255W and vacuum cleaner(shiftable)/1.07kW in R3, microwave oven(shiftable)/1.04kW and rice cooker (shiftable)/1.03kW in R4. The non-shiftable HVAC (heater/1.16kW, ventilation fan/60W, and air-conditioner/1.2kW) is installed in every room. Probabilistic use of specific electric appliance is described by emission probability. The emission probability $p^e_{i,j}$ shown in Fig.3(c) can be expressed as

$$\sum_{j=1}^{l_i} p^e_{i,j} = 1, \quad p^e_{i,j} > 0 \quad (2)$$

where i = room number and j = index of the appliance in the room i and l_i = number of electric appliances in the room i. The probabilistic use of each electric appliance over time is determined by the Korean time-use survey (KTUS) data [10] obtained by the Korea Power Exchange with 500 residences. Figure 4 shows the temporal use of 12 electric appliances, e.g., 9 shiftable and non-shiftable electric appliances plus 3 HVAC appliances. The data of probabilistic use are transformed into emission probabilities that determine which electric appliance will be used for 10 minutes. For instance, the probability of watching TV at 8 PM is 0.27 and the probability of using an iron at 8 PM is 0.03, according to the KTUS data. Therefore, the conditional emission probabilities of watching TV and using iron, on the condition that the resident is present in room R1, are 0.27/(0.27+0.03) and 0.03/(0.27+0.03), respectively, where 0.27+0.03 is the normalizing sum for the room R1. Therefore, the resident behavior during 10 minute time interval consists of transition (between rooms) followed by the use of the electric appliances in the room that the resident enters at the beginning of the 10 minute time interval. The operation of HVAC can be set to depend on resident location. When the operation of HVAC is controlled according to

resident location, differentiated(tight) operating condition of HVAC is applied for the room, where the resident is located, as shown in Fig.3(a). For instance, in the summer, the target temperature of the room with the resident can be set lower than those of other rooms. Similarly, another component determining living comfort, the air quality measured by CO_2 density in the room, can be controlled according to the resident location. When the resident enters a room in the beginning of a time interval, according to the transition probability of Markov chain model, target temperature and target CO_2 density are adjusted, following the operation scenario of HVAC for the room where the resident is located, and HVAC initiates operation to meet the target temperature and target CO_2 density. If target temperature and target CO_2 density are already met before resident entrance, HVAC is in idle mode. The HVAC in a room without the resident is also operated when the target temperature and target CO_2 density for the room without resident are not met. When the target temperature and target CO_2 density for the room without resident are close to those for the room where resident is located, living comfort of the resident is maintained regardless of temporal transition of resident location.

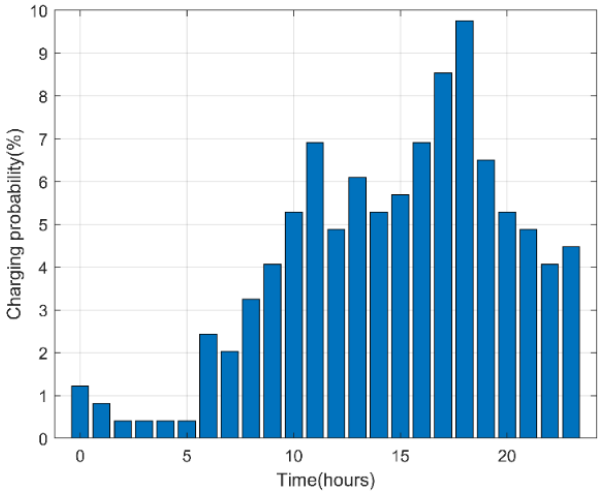

FIGURE 2. Charging probability p_c (n_h) (%) of an EV over a day. The sum of charging probabilities is 100%.

Charging probability of EV in TABLE 1 indicates the probability(%) of an event that an EV initiates charging in the beginning of each hour. The EV is charged before being discharged for reduction of total power consumption. For a nanogrid consisting of 3 houses, 3 EVs are connected in V2H configuration. When the time for initiation of charging is taken as a random variable, 3 random variables of 3 EVs are independent and identically distributed. The charging probability listed in TABLE 1 can be graphically shown as Fig.2. Probability mass at k hrs represents charging probability over 1 hour time zone starting from k hrs. Charging probability is obtained from 6,080 EVs registered in Jeju Island. The EV connected to the charger can take three different modes: charging mode, discharging mode, and idle mode. When it is in charging (discharging) mode, it is charged(discharged). Random initiation of EV charging can be modeled by charging probability $p_c(n_h)$. Time-varying $p_c(n_h)$ in % obtained from the EVs registered in Jeju Island, Korea is specified in TABLE 1. It is seen in TABLE 1 that the charging probability $p_c(n_h)$ is the highest at around 6 PM when the resident returns from work.

TABLE 1. Charging probability $p_c(n_h)$ (%) of an EV varying over one day. The sum of charging probabilities is 100%.

TIME ZONE	00:00~ 01:00	01:00~ 02:00	02:00~ 03:00	03:00~ 04:00	04:00~ 05:00	05:00~ 06:00
CHARGING PROBABILITY	1.2195	0.813	0.4065	0.4065	0.4065	0.4065
TIME ZONE	06:00~ 07:00	07:00~ 08:00	08:00~ 09:00	09:00~ 10:00	10:00~ 11:00	11:00~ 12:00
CHARGING PROBABILITY	2.439	2.0325	3.252	4.065	5.2846	6.9106
TIME ZONE	12:00~ 13:00	13:00~ 14:00	14:00~ 15:00	15:00~ 16:00	16:00~ 17:00	17:00~ 18:00
CHARGING PROBABILITY	4.878	6.0976	5.2846	5.6911	6.9106	8.5366
TIME ZONE	18:00~ 19:00	19:00~ 20:00	20:00~ 21:00	21:00~ 22:00	22:00~ 23:00	23:00~ 00:00
CHARGING PROBABILITY	9.7561	6.5041	5.2846	4.878	4.065	4.4715

III. PREDICTIVE POWER MANAGEMENT

Predictive power management consisting of PV power production predicted by the LSTM network and consequent power management by the genetic algorithm (GA) [45] is presented. Global optimization minimizing electricity cost over the entire time interval, e.g., 24hrs in this work, is impractical due to the following reasons. Firstly, the specific time of EV charging/discharging is unknown at the current time interval. Secondly, realized uses of electric appliances subject to emission probabilities in the future of the day are unknown at the current time interval. Therefore, optimization for the current time interval provides locally optimal results valid with given operating conditions. Each operating condition can be taken as a parameter affecting power management. Two operating conditions are principally considered in this work for power management, due to their relatively high power level. PV power production significantly affects the power supply of the grid. When PV power, which is the primary power used ahead of grid power, is sufficient, the electricity cost incurred by grid power consumption is low. It is legitimately assumed that the operating cost of PV panels is 0. Hence, the level of PV power production in the current time interval and beyond is a critical concern. EV charging/discharging is also very important for efficient power management, due to the large power

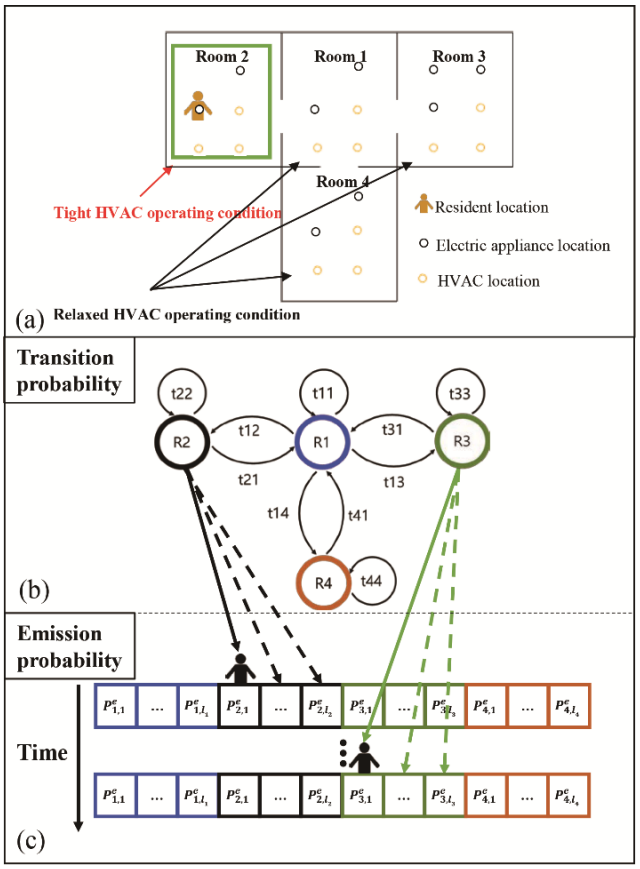

FIGURE 3. Operating condition of HVAC according to resident location and Markov chain model for resident behavior: (a) operating condition of HVAC according to resident location; (b) transition probability for resident location; (c) emission probability for using an electric appliance in each room.

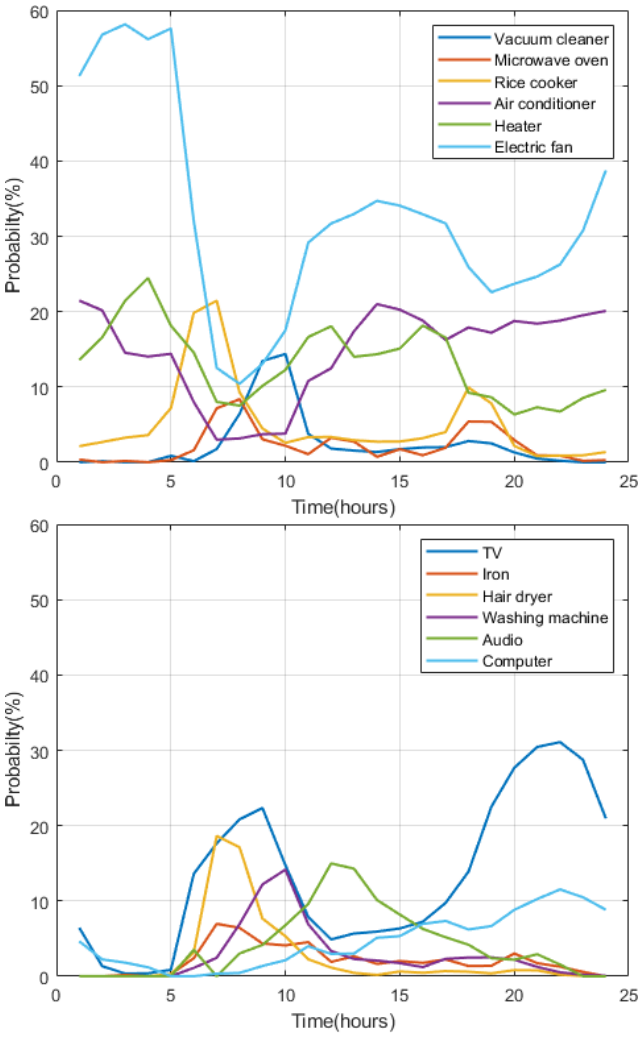

FIGURE 4. Temporal use of TV, iron, hair dryer, washing machine, audio, computer, vacuum cleaner, microwave oven, rice cooker, air-conditioner, heater, and electric fan on weekdays [10].

consumed/provided by the EVs. Since EVs are another power source when discharging, timely control of EVs contributes to reduction of time dependent electricity cost. Considering that EV modes are determined by power budget as well as PV power production, it is important to take (near) future PV power production into account for the choice of EV mode. If future PV power production is successfully predicted and taken into account for power management, consequent predictive power management can provide enhanced results of power management.

In this section, a multi-objective optimization framework for power management is presented and details of the LSTM network for prediction of PV power production are described, followed by methodology on how to choose EV modes based on predicted PV power production.

A. MULTI-OBJECTIVE OPTIMIZATION BY GA FOR POWER MANAGEMENT

The type of optimization for presented power management is multi-objective optimization. Multi-objective optimization involves simultaneous minimizations or maximizations or mixed optimization of multiple objective functions that are dependent on a set of constraints [48]. The goal is to solve complex optimization problems by simultaneously considering potentially conflicting objectives. Many real-world engineering challenges involve several objectives such as cost, performance, and reliability. In this paper, the GA is used to solve multi-objective optimization relevant to nanogrid power management. Technical details of the GA are referred to [45].

Due to the availability of specific technical information of electric appliances in nanogrid, power management of individual electric appliances is possible with the nanogrid. The objective functions of nanogrid power management are the electricity cost associated with grid power consumption and the scheduling delay of shiftable electric appliances and EV charging/discharging. Power management for the nanogrid is associated with the DR program and EVs can be classified as shiftable appliances. From this standpoint, the multi-objective optimization can be expressed

as follows

$$
\begin{aligned}
&\textit{minimize electricity cost at the } n-\textit{th time interval}\\
&= \min EC(n)\\
&= \min[PW(n) - PW^{PV}(n)] * C(n)\\
&= \min[\sum_{EV=1}^{M} PW_{EV}(n) * O_{EV}(n)\\
&\qquad + \sum_{a=1}^{N_A^{nano}} PW_a(n) * O_a(n) - PW^{PV}(n)] * C(n)\\
&= \min_{O_{EV}(n),EV=1,..,M,O_k(n),k=1,..,S}\\
&\quad \times \left[\begin{array}{l} \sum_{EV=1}^{M} PW_{EV}(n) * O_{EV}(n)\\ + \sum_{k=1}^{S} PW_k^{shiftable}(n) * O_k(n) \end{array} \right] * C(n)\\
&\quad + \left[\begin{array}{l} \sum_{i=1}^{N_1} PW_i^{HVAC}(n) * O_i(n)\\ + \sum_{j=1}^{N_2} PW_j^{non-shiftable}(n) * O_j(n)\\ -PW^{PV}(n) \end{array} \right] * C(n)\\
&\textit{minimize Total delay at the } n-\textit{th time interval}\\
&= \min Total\_delay(n)\\
&= \min_{O_{EV}(n),EV=1,..,M,O_k(n),k=1,..,S} \left[\begin{array}{l} \sum_{EV=1}^{M} O_{EV}(n) * d_{EV}(n)\\ + \sum_{k=1}^{S} O_k(n) * d_k(n) \end{array} \right] \qquad \text{(3a)}
\end{aligned}
$$

subject to

$$
\begin{aligned}
&\left[\begin{array}{l} \sum_{EV=1}^{M} PW_{EV}(n) * O_{EV}(n)\\ + \sum_{a=1}^{N_A^{nano}} PW_a(n) * O_a(n) - PW^{PV}(n) \end{array} \right] < PW^{\max}\\
&d_{EV}(n) \le d_{EV,\max} \quad EV = 1, .., M\\
&d_k(n) \le d_{Shiftable,\max} \quad k = 1, \ldots, S \qquad \text{(3b)}
\end{aligned}
$$

where $PW(n)$ is the total power consumption and $PW(n) - PW^{PV}(n)$ is the grid power consumption and $PW^{\max}$ is the maximum power consumption allowed by the grid and $C(n)$ is the rate of electricity based on the DR program and $PW^{PV}(n)$ is the PV power production. The $PW_{EV}(n)$, $PW_a(n)$ are the power consumption of the EV-th EV, a-th appliance (S shiftable appliances, N_1 non-shiftable appliances other than HVAC, N_2 non-shiftable HVAC), respectively. The $O_{EV}(n)$, $O_a(n)$, $O_k(n)$ are the on-off switching functions of the EV-th EV, a-th appliance, k-th shiftable appliance, respectively. Note that $N_A^{nano} = S + N_1 + N_2$.

The 1st term in (3a) indicates electricity cost caused by the power consumption of EV. When switching function $O_{EV}(n) = -1$, the EV discharges(provides) electric power and contributes to reduction of electric cost. When switching function $O_{EV}(n) = +1$, the EV is charged, consuming electric power like an electric appliance. With $O_{EV}(n) = 0$, the EV is in idle mode. Charging/discharging condition of an EV is mathematically expressed in (5b). The 2nd term in (3a) indicates electricity cost caused by the power consumption of shiftable appliances. These two terms are to be minimized to minimize the electric cost. Electric cost associated with the remaining 3 terms in (3a) cannot be minimized by multi-objective optimization. They are given according to resident behavior(non-shiftable appliances), HVAC control mode, and PV power production. Total delay in (3a) consists of scheduling for EV charging/discharging and shiftable appliances. Goal of scheduling is to minimize total delay. The switching function $O_{EV}(n)$ is set by (5a) or (5b) prior to the use of it for (3a) and (3a). However, when the $O_{EV}(n)$ in conjunction with other switching functions in (3a), (3a) violates the constraint occasionally, the GA(Genetic Algorithm) changes its value to one of other two possible values.

The scheduling delays of the EV-th EV charging and use of the k-th shiftable appliance, defined as $d_{EV}(n)$ and $d_k(n)$, respectively, are increased by 1 when the EV charging or use of the shiftable appliance is delayed to the next time interval and becomes 0 when actually charged or used. Scheduling delay is measured for each request. Therefore, multiple requests for specific shitable appliance are associated with their respective delays. Since the EV charging and use of the shiftable appliance can be requested multiple times, $d_{EV}(n)$ and $d_k(n)$ in (3a) represent the sum of individual delays measured for each EV and shiftable appliance, respectively. The entire EV charging process of an EV is decomposed into distinct partial charging processes over different time intervals, each representing a request for 10 minute charging. Each partial charging over 10minutes is independently scheduled just like a shiftable appliance. For instance, when the first partial charging of the EV-th EV at the n-th time interval is postponed to the next interval, the $d_{EV}(n+1)$ is increased by 1. If the first partial charging is postponed again at the $(n+1)$-th time interval, $d_{EV}(n+2)$ will be increased by 3 due to 2 of the first partial charging and 1 of the second partial charging. The delay of the first partial charging becomes 0 ahead of the second partial charging when the EV-th EV undergoes a partial charging. When an EV is discharged at the n-th time interval, e.g., partial discharging, according to the value of switching function $O_{EV}(n)$, an additional partial charging process associated with a delay is considered created at the time interval. It is because full charging requires one more partial charging to make up the lost energy due to partial discharging. Total number of partial charging processes of an EV required for full charging, therefore, depends on its initial SOC and the number of partial discharging processes before full charging.

The sum of individual delays measured for each EV should be less than or equal to $d_{EV,\max}$ and the sum of individual delays measured for a shiftable appliance should be less than or equal to $d_{Shiftable,\max}$.

Electricity cost function $EC(n)$ composed of individual costs of EVs and electric appliances should be minimized to decrease electricity cost. Total delay at the n-th time interval $Total\_delay(n)$ consisting of EVs and shiftable electric appliances should also be minimized to complete delayed uses as soon as possible. Therefore, simultaneously minimizing these two objectives is a conflicted optimization and the result of the optimization is a trade-off solution between marginally optimal solutions. The power generated by PV panels is used before the grid power to lower the electricity cost EC(n). When the total power consumption is lower than the PV power production, remaining power can be used to charge EV(s).

The indoor/outdoor temperature and CO_2 concentration are related to HVAC control. The indoor temperature $T^r_{in}(n+1)$ and CO_2 concentration $CO^r_{2\,in}(n+1)$ of the r-th room at the $(n+1)$-th time interval are determined according to the operation of air-conditioner in summer (or heater in winter) and ventilation fan, which are given in relation to $T^r_{in}(n)$ and $CO^r_{2\,in}(n)$ at the n-th time interval, respectively, as follows [49]

$$T^r_{in}(n+1) = \begin{bmatrix} T^r_{in}(n) + 0.0145 O^r_{VF}(n)[T_{out}(n) - T^r_{in}(n)] \\ -0.378 O^r_{AC}(n) + 0.0195[T_{out}(n) - T^r_{in}(n)] \end{bmatrix} \quad (4a)$$

$$CO^r_{2\,in}(n+1) = CO^r_{2\,in}(n) + 1.075 O^r_{VF}(n)[CO_{2\,out}(n) - CO^r_{2\,in}(n)] \quad (4b)$$

where $T_{out}(n)$ indicates the outdoor temperature at the n-th time interval and $CO_{2\,out}(n)$ represents outdoor CO_2 concentration at the n-th time interval and $O^r_{VF}(n)$, $O^r_{AC}(n)$ are $O_i(n)$ of a ventilation fan, air-conditioner, respectively, installed in the r-th room.

B. LSTM NETWORK FOR PREDICTION OF PV POWER PRODUCTION

Recursive neural network (RNN) is a special kind of feed-forward neural network which is useful for modeling time-sensitive sequences. At each time, the RNN receives input from the current example and also from the hidden layer of the previous state. The output is calculated for the given hidden state at that time stamp. The hidden state acts as the memory of the RNN. It holds information on previous data that the network has seen before. Because of the connection between sequential states, the output at each time is indirectly associated with all the previous inputs. In long-range sequences, the simple RNN architecture suffers from a vanishing gradient problem that causes the RNN to forget important information over the chain. The LSTM network addresses this problem by re-parameterizing the RNN. The main idea of the LSTM network is introducing three gates (forget gate, input gate, and output gate) to control the data flow in the RNN. Figure 5 shows the architecture of LSTM network for prediction of PV power production. It is noted that the Markov chain model in Fig.3 is not related to use of the LSTM network. As shown in Fig.5(a), the LSTM network consists of the LSTM layers, fully connected layers, and the output layers. The LSTM layers are built up with interconnected LSTM cells, each composed of the three gates as depicted in Fig.5(b). The forget gate scales down the internal state of the cell before adding it as input to the cell through the self-recurrent connection of the cell, therefore adaptively forgetting or resetting the cell's memory. The input gate controls the flow of input activations into the LSTM cell and the output gate controls the output flow of cell activations into the neighbored and connected cells. As a result, the structure of the LSTM network prevents the vanishing gradient of the long-term dependencies. The detailed architecture shown in Fig. 5 follows the one proposed in [34].

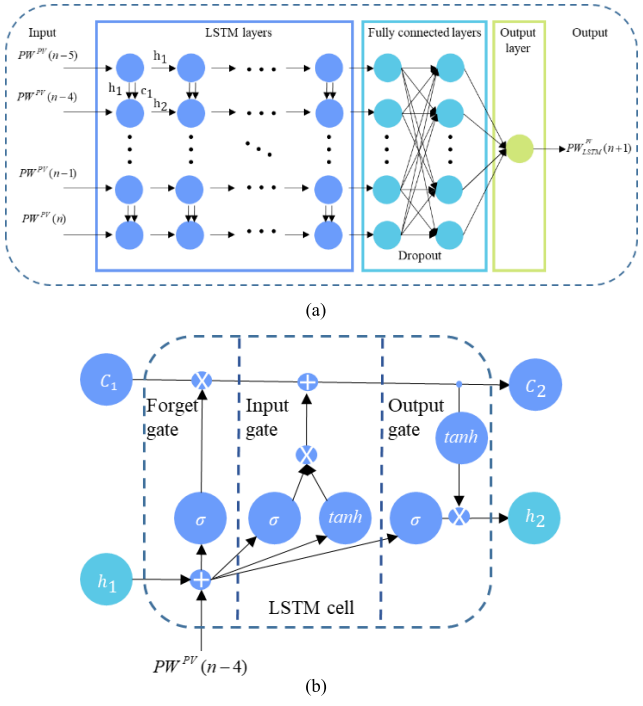

FIGURE 5. Architecture of LSTM network: (a) LSTM layers and fully connected feed-forward layers; (b) LSTM cell.

Figure 6 shows a sample of daily PV power production of a nanogrid with maximum achievable production 6kW. Since PV power production is important for power management, variation of PV power production should be taken into account. When temporal trend of PV power production rises, more electric appliances are likely to consume power in current and next time intervals. In case of EVs, the EV mode is likely to be charging, rather than discharging. For predicting the PV power production, the LSTM network with 6 LSTM layers and 2 fully connected layers is proposed as shown in Fig.5(a). Input data applied to the

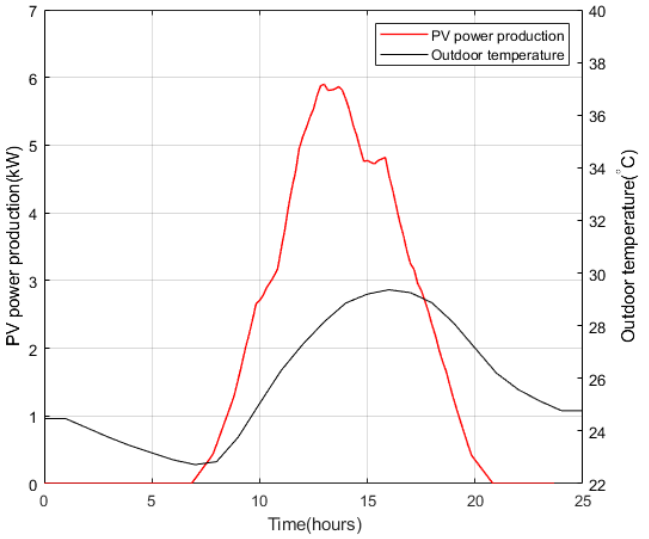

FIGURE 6. Samples of daily PV power production of a nanogrid consisting of 3 houses and daily variation of outdoor temperature in the summer season in Korea.

first LSTM layer are $PW^{PV}(n-i)$, where $i = 0, \ldots, 5$. The number of LSTM layers and the number of input data to the first LSTM layer are determined by trial-and-error method. Prediction performance of PV power production measured by root-mean-squared-error is among the best with 6 input data and 6 LSTM layers. The root-mean-squared-error(RMSE) of PV power production obtained with 1 year PV power production dataset is about 9% with 6 inputs of the input layer(first LSTM layer) and 6 LSTM layers. Occasionally, prediction error becomes upto 14%. Similar level of prediction performance of the LSTM network is reported in [50]. The 9% represents 0.5kW for the nanogrid consisting of 3 houses and capable of 6kW PV power production. The prediction error becomes higher with bad weather conditions such as cloudy days and rainy days, as noted in [51]. The number of LSTM layers and the number of input data to the input layer are determined by trial-and-error method like other works [52] dealing with LSTM network. When the number of LSTM layers is not properly set, inherent parameters of the LSTM network grow or shrink exponentially and eventually become inadequate for the training data. It is found that for 6 LSTM layers prediction performance measured by RMSE value is the best with the number of inputs 6 when the range of the number of inputs is 5∼15. More input data and/or more LSTM layers are found to give a marginal impact on the improvement of prediction performance. During supervised learning of the LSTM network with historical data of PV power production, the desired output datum of the LSTM network for predictive power management is the PV power production in the next time interval $PW^{PV}_{LSTM}(n+1)$. During validation and testing $PW^{PV}_{LSTM}(n+1)$ will be predicted PV power production. It is noted that the number of present and past inputs $PW^{PV}(n-i)$ determines the range of past samples accounted for predicted $PW^{PV}_{LSTM}(n+1)$. Dropout is applied to fully connected layers to prevent local optima in the prediction of $PW^{PV}_{LSTM}(n+1)$. Values of the initial learning rate, dropout rate, and gradient threshold are hyperparameters tuned for the prediction performance and these for simulations are presented in Section IV. The structure of an LSTM cell is shown in Fig.5(b) corresponding to the input $PW^{PV}(n-4)$ Note that the LSTM cell in Fig.5(b) is rotated as much as 90° in counter-clockwise direction as compared to that in Fig.5(a) and the cell state c_2 and hidden state h_2 in Fig.5(b) are evaluated according to relevant processing steps. The $tanh(\cdot)$, $\sigma(\cdot)$ in Fig.5(b) represent a hyperbolic tangent function, sigmoid function, respectively. Details of the processing steps are referred to [53].

C. EV CHARGING AND DISCHARGING WITH PV POWER

The EV modes of the EV-th EV can be described by the switching function $O_{EV}(n)$. When the EV modes are determined by the grid power consumption $PW(n)$-$PW^{PV}(n)$ and SOC, they can be typically presented by the $O_{EV}(n)$ as follows

$$O_{EV}(n) = \begin{cases} -1\,(discharging) & if\ (PW(n)-PW^{PV}(n) > PW^{\max}) \\ & \quad and\ (SOC_{EV}(n) > SOC_{\min}) \\ 1\,(charging) & if\ (PW(n)-PW^{PV}(n) < PW^{\max}) \\ & \quad and\ (SOC_{EV}(n) < SOC_{\max}) \\ 0(idle) & otherwise \end{cases} \tag{5a}$$

where $SOC_{EV}(n)$, SOC_{min}, SOC_{max} represent the SOC at the n-th time interval, minimum allowed SOC of the EV, maximum allowed SOC of the EV, respectively, and $SOC_{EV}(n)$ is always adjusted between SOC_{min} and SOC_{max}.

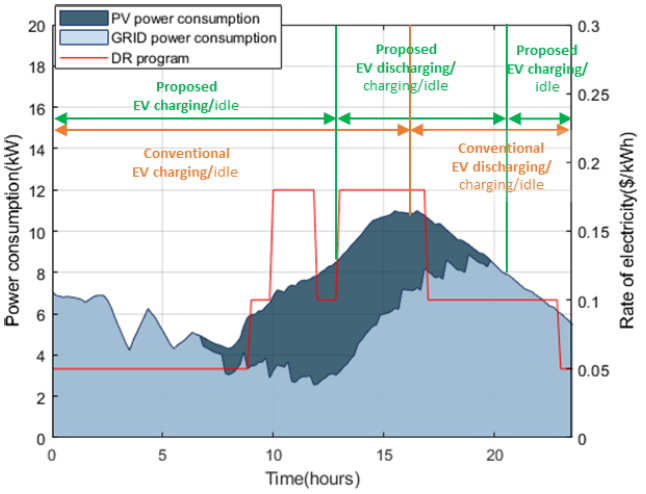

FIGURE 7. Total power consumption of HVAC, shiftable, and non-shiftable electric appliances and time zones for EV charging, discharging, and idle modes according to the switching conditions in (5a), (5b). $PW^{\max} = 7$kW.

Figure 7 shows power consumption of all electric appliances, excluding EVs, of the nanogrid consisting of 3 houses.

TABLE 2. Operating conditions of simulations.

Simulation number	Number of houses in nanogrid	HVAC-control (Yes=O/No=X)	Scheduling	Maximum PV power production at each house	EV discharging with LSTM network	Number of appliances (S=Shiftable/N_1=Non-Shiftable/N_2=HVAC)
#1	3	O or X	O or X	2kW	O or X	S=21, N_1=6, N_2=36
#2	10	O or X	O or X	2kW	O or X	S=70, N_1=20, N_2=120
#3	3	O	O	1kW or 2kW	O or X	S=21, N_1=6, N_2=36
#4	3	O	O	2kW	O	S=21, N_1=6, N_2=36

It is noted that the peak power consumption in Fig.7 is due to large power consumption of HVAC caused by high outdoor temperature. When pattern of temporal use shown in Fig.4 is changed to some extent, representing different grid loading, it is expected that profile of total power consumption with the same HVAC operation plan is not significantly changed. It is because the scheduling of shiftable appliances consuming electric power much more than non-shiftable appliances can distribute power consumption of them over time. Part of total power consumption $PW(n)$(=PV power consumption+GRID power consumption) is offered by PV panels and the rest is supplied by the grid. Variation of power consumption of electric appliances, other than EVs, is determined by the resident behavior characterized by the Markov chain model and KTUS data. Figure 7 also shows the rate of electricity specified by a DR program. The DR program initiated by the Korea Electric Power Corporation (KEPCO) applies \$0.05/kWh over the time period of 23:00∼09:00, \$0.1/kWh over the time periods of 09:00∼10:00, 12:00∼13:00, 17:00∼23:00, and \$0.18/kWh over the time periods of 10:00∼12:00, 13:00∼17:00 [22]. Peak of total power consumption is seen to occur at around 16hrs, which corresponds to high rate of electricity. Based on the distribution of power consumption over time in Fig.7 and the conventional EV charging/discharging policy in (5a), the peak load is reduced by EV discharging (with occasional charging) around 20hrs following EV charging. Note that the main purpose of EV discharging in (5a) is to reduce grid power consumption $PW(n) - PW^{PV}(n)$, which is not free. On the other hand, rate of electricity is rather low during 17hrs-23hrs, representing that the conventional EV discharging policy is not cost-effective. Without PV power production, peak grid power consumption at 20hrs would shift to around 16hrs and cost reduction becomes more significant with EV discharging. Therefore, the switching function $O_{EV}(n)$ should be modified in the presence of PV power.

In order to reduce electricity cost in the presence of PV power, different EV charging/discharging policy is established. The total electricity cost over 24hrs is more efficiently reduced by executing EV discharging over time zones 10:00∼12:00, 13:00∼17:00, where the PV power production is decently high as seen in Fig.6. Since PV power production is considerably high over the time zones of high electricity cost, the EV charging/discharging policy can take advantage of the pattern of PV power production. For predictive power management with the LSTM network, the switching function $O_{EV}(n)$is modified as follow

$$O_{EV}(n) = \begin{cases} -1\,(discharging) & \begin{array}{l} if\ \{(PW(n)-PW^{PV}(n) > PW^{\max}) \\ \quad and\ (SOC_{EV}(n) > SOC_{\min})\} \\ or\ \{(PW^{PV}(n) > PW^{PV}_{LSTM}(n+1)) \\ \quad and\ (T_{out}(n) > T_{in,tar}) \\ \quad and\ (SOC_{EV}(n) > SOC_{\min})\} \end{array} \\ 1\,(charging) & \begin{array}{l} if\ (PW(n)-PW^{PV}(n) < PW^{\max}) \\ \quad and\ (SOC_{EV}(n) < SOC_{\max}) \\ and\ (PW^{PV}(n) < PW^{PV}_{LSTM}(n+1) \\ \quad or\ T_{out}(n) < T_{in,tar}) \end{array} \\ 0\,(idle) & otherwise \end{cases} \tag{5b}$$

where $T_{in,tar}$ represents required indoor temperature, e.g., temperature in rooms, effective to all rooms where the resident is not located. The $T_{in,tar}$ is achieved by proper HVAC operation. For simplicity of notation, $PW^{PV}_{LSTM}(n+1)$ is used in (5b) as the predicted $PW^{PV}_{LSTM}(n+1)$. Charging condition in (5b) is tighter than the charging condition in (5a) whereas discharging condition in (5b) is more relaxed as compared to the discharging condition in (5a). Therefore, the switching function $O_{EV}(n)$ in (5b) is more inclined to discharging, which is beneficial for reduction of electricity cost. The first condition of EV discharging $(PW(n) - PW^{PV}(n) > PW^{\max})$ *and* $(SOC_{EV}(n) > SOC_{\min})$ indicates emergency-based EV discharging while the second condition $(PW^{PV}(n) > PW^{PV}_{LSTM}(n+1))$ *and* $(T_{out}(n) > T_{in,tar})$ *and* $(SOC_{EV}(n) > SOC_{\min})$ represents policy-based EV discharging. The first condition of EV discharging is already taken into account by the constraint of the GA. The trend of PV power production can affect the switching function $O_{EV}(n)$, because falling PV power production, i.e., $PW^{PV}(n) > PW^{PV}_{LSTM}(n+1)$, can be compensated by EV

discharging and rising PV power production leaves room for EV charging. The indoor temperature in relation to outdoor temperature can affect the EV mode, because the HVAC is installed in every room and causes significant power consumption. When the outdoor temperature is higher than the target indoor temperature, the air-conditioner is on and the EVs are more likely to be discharged. Therefore, the condition $T_{out}(n) > T_{in,tar}$ works like $PW(n) - PW^{PV}(n) > PW^{\max}$ in (5a) and often indicates peak total power consumption. When comparing discharging condition in (5a) with that in (5b), EV discharging condition in (5b) occurs regardless of $PW(n)$ relative to $PW^{\max}$, representing that excessive amount of power $PW(n) - PW^{PV}(n)$ is supplied by the EVs. The discharging condition in (5b) corresponds to most 10 time intervals in the time zone 13:00∼17:00, where the rate of electricity is high and the total power consumption is decently large and PV power production is in falling trend. Over the time zone 10:00∼12:00, power consumption of electric appliances is not large and effectively managed by the PV power, as seen in Fig.7. Thus, reduction of electricity cost is less significant in this time zone. The EV charging occurs if $(PW^{PV}(n) < PW^{PV}_{LSTM}(n+1)\ or\ T_{out}(n) < T_{in,tar})$, in addition to the charging condition in (5a). This additional condition represents time zones before 12hrs and (potentially) after 20hrs, as suggested by Fig.6. For other cases of switching conditions, the $O_{EV}(n)$ is set to idle mode. Thinner words in Fig.7 following "/" indicate less frequent operation, as compared to the operation marked by thicker words.

The $O_{EV}(n)$ obtained in (5b) is used as the $O_{EV}(n)$ in (3a), (3a). When the $O_{EV}(n)$ in conjunction with other switching functions in (3a), (3a) violates the constraint occasionally, the GA changes its value to one of other two possible values.

IV. SIMULATION RESULTS

In this section, simulation results of the proposed power management scheme and other schemes are presented.

A. SIMULATION SETUP

Daily variation of PV power production of a nanogrid consisting of 3 houses and the daily variation of outdoor temperature shown in Fig.6 are used for simulations. The maximum achievable PV power production of rooftop PV panels at each house in Fig.6 is 2kW. For some simulations with the maximum PV power production at each house set to 1kW, half the PV power production in Fig.6 is taken at each time. Two types of nanogrids are used for simulations. Smaller nanogrid consists of 3 houses and larger nanogrid is composed of 10 houses. For the smaller nanogrid, $PW^{\max}$ is set to 9kW and for the larger nanogrid $PW^{\max}$ is set to 27kW, unless stated otherwise. Considering the power ratings of electric appliances, including HVAC, and charging rate of an EV, 9kW and 27kW of $PW^{\max}$ are considered tight or moderately tight. The battery capacity of EV is 15kWh which is close to that of compact EV in the market. The charging rate for each EV is either 3kW or 6kW and EV charging/discharging efficiency is 90%. Since charging rate 3kW or 6kW for the EV battery of 15kWh capacity takes 5hrs or 2.5hrs for full charging, charging considered in our work is a slow charging. The discharge rate is set to 0.33C(=1kW), considering the state of health, as indicated in [54]. In simulations, depth of discharge (DOD) of EV is within the range 10%∼20%. These numbers of discharge rate and DOD fall into ranges suitable for state of health [54]. Due to the low discharge rate and low range of DOD, adversary effect of EV charging/discharging on EV battery is seen to be minor. Also, SOC range 20%-80% considered in simulations does not correspond to undercharging and overcharging that causes reduced lifespan of EV battery [55]. When discharging, all EVs with SOC allowing it discharge at the same time, similar to the manner in [54]. The DR program by the KEPCO is used for evaluation of electricity cost. The details of simulations #1∼#4 are listed in TABLE 2. As described in Section II above (2), the numbers of shiftable appliances, non-shiftable appliances, HVAC appliances in each house are 7, 2, 12, respectively. Thus, for instance, the number of shiftable appliances S in the nanogrid of 3 houses is 7*3=21. Two modes of HVAC operation are considered. In HVAC-control mode, target temperature in one of the 4 rooms in each house, where the resident is located, is 23 degrees and the target temperature for other rooms is 25 degrees, which represents the $T_{in,tar}$ in (5b). In no-HVAC-control mode, the target temperature in all four rooms in each house is 23 degrees. Due to the large power consumption of HVAC to keep the temperature in all rooms at 23 degrees, $PW^{\max}$ is not set for the scheme relevant to this mode. The outdoor CO_2 concentration is set to 550 ppm throughout the day and the target CO_2 concentration in each room is set to 500 ppm regardless of the resident location. Since the power rating of the ventilation fan is much less than that of air-conditioner, the adjustment of target CO_2 concentration according to resident location does not make a big difference in power consumption.

The training parameters of the LSTM network, shown in TABLE 3, are as follows. The total number of training epochs is 1000 and batch size is 200 and the ADAM [56] optimization algorithm is used with learning rate 0.005, gradient moving average 0.9, dropout rate 0.2, and gradient threshold 1 [36], [57]. Inadequate learning rates might cause an undesirable local minimum and overfitting. Dropout and gradient are used to prevent the local minima. The dataset of PV power production collected during 1 year is split into 80 percent for training and 20 percent for validation. Daily variation of PV production in Fig.6 is an entry of the validation dataset. The parameters of the GA used for the multi-objective optimization are crossover probability 0.8, mutation probability 0.01, the maximum number of generations 100, and population size 100. The initial and common SOC of EVs is assigned as 20%, corresponding to deplete state of the battery. The initial SOC of EVs in each simulation is set to common for all schemes. The $d_{EV,\max}$ for full charging of an EV is set to 12hrs, just

TABLE 3. Parameters related to training and validation of LSTM network.

Parameter	Value	Parameter	Value
Training epochs	1000	Number of PV power production samples used for training	(365*0.8)*24*6
Batch size	200	Number of PV power production samples used for validation	(365*0.2)*24*6
Initial learning rate	0.005	Gradient threshold	1
Dropout	0.2	Gradient moving average	0.9
Optimizer	ADAM		

like the constraint $d_{Shiftable,\max}$ on other shiftable appliances. For each 10% increment of SOC, 2.5kWh charging is taken necessarily. With a rate of charging 3kW, full charging, corresponding to the SOC 80%, takes 5hrs when initial SOC is 20%. Conditions on charging and discharging of EVs are in (5a), (5b).

Simulation #1 is to see the effect of EV charging/discharging on nanogrid power management with 3 houses. Simulation #2 is to observe the effect of EV charging/discharging on nanogrid power management with 10 houses. Simulation #3 is to see the effect of the level of PV power production on nanogrid power management. In simulation #4, different rates of EV charging are considered for nanogrid power management. Since initial charging according to charging probability should not occur too late to complete within 24hrs full charging of EVs, simulations providing successful completion of full charging of all EVs by all schemes in 24hrs are only presented. Note that the EVs of the proposed scheme corresponding to (5b) discharge earlier than those of the conventional scheme pertinent to (5a), as suggested in Fig.7. Therefore, the conventional scheme always has more time for charging and therefore highly likely more energy reserved for discharging. The summary of the simulation results in terms of the electricity cost is at the end of this section.

B. SIMULATIONS

Simulation #1: Effect of EV charging/discharging on the operation of nanogrid consisting of 3 houses with PV power production.

Figure 8 presents the power consumption according to 4 different power management schemes. The total power consumption in Fig.8(a) represents grid power consumption $PW(n) - PW^{PV}(n)$ in (3a). The maximum achievable PV power production of rooftop PV panels of each house is 2kW. The PV power is used ahead of grid power and thus the grid power is used only when $PW(n) - PW^{PV}(n) > 0$. The "no-scheduling+no-HVAC-control" scheme represents the power management in no-HVAC-control mode without scheduling of shiftable appliances. The "scheduling+HVAC-control" scheme indicates the power management in HVAC-control mode with the scheduling of shiftable appliances. With the "no-scheduling+no-HVAC-control" scheme and "scheduling+HVAC-control" scheme, EVs are charged up to 80% and do not discharge for power consumption of electric appliances. The "scheduling + HVAC-control + EV-ch/disch" scheme implies that the EVs are charged/discharged according to the conditions in (5a), while the "scheduling + HVAC-control + EV-ch/disch + LSTM" scheme represents that the EVs are charged/discharged following (5b).

The peak load in the "no-scheduling+no-HVAC-control" scheme is higher than other cases because for this case the target temperature of all rooms is 23 degrees, regardless of resident location, and electric appliances are used without any scheduling. The "scheduling+HVAC-control" scheme represents that shiftable appliances are scheduled by the GA and the HVAC is controlled to get 23 degrees in the room where the resident is located and 25 degrees for the other 3 rooms. The "scheduling+HVAC-control+EV-ch/disch" scheme performs EV discharging to reduce peak load at around 20hrs which corresponds to low rate of electricity. The "scheduling+HVAC-control+EV-ch/disch+LSTM" scheme for predictive power management with LSTM network, however, executes EV discharging around 15hrs when the rate of electricity is high, thereby causing significant reduction of electricity cost. It is seen in Fig.8(a) that the grid power consumption can be 0 with the "scheduling+HVAC-control+EV-ch/disch+LSTM" scheme, due to EV discharging process in Fig.8(c). Due to different conditions on EV charging/discharging, two schemes show significantly different total power consumption before 15hrs and around 20hrs. Since $PW^{\max}$ 9kW with decent amount of PV power is sufficiently large, the total delay incurred by scheduling of shiftable appliances is negligible and thus the variation of power consumption of $S + N_1$ shiftable and non-shiftable appliances according to each scheme is close to each other, as shown in Fig.8(b). Unlike Fig.8(a), portion of power consumption in Fig.8(b) comes from PV power. Therefore, Figure 8(b) shows true power consumption of $S+N_1$ shiftable and non-shiftable appliances.

EV charging/discharging by the "no-scheduling+no-HVAC-control" scheme in Fig.8(c) shows initiation of EV charging according to charging probability. Initiation of charging the first EV occurs at 10hrs, the second EV at 11hrs, and the third at 13hrs, since stepwise increment of power consumption of EV charging occurs at these timings. Similarly to Fig.8(b), portion of EV charging power in Fig.8(c) comes from PV power and the rest from the grid. It is seen in Fig.8(c) that by the "scheduling+HVAC-control+EV-ch/disch+LSTM" scheme the EVs are charged until 13hrs and then discharged to save electricity cost, whereas by

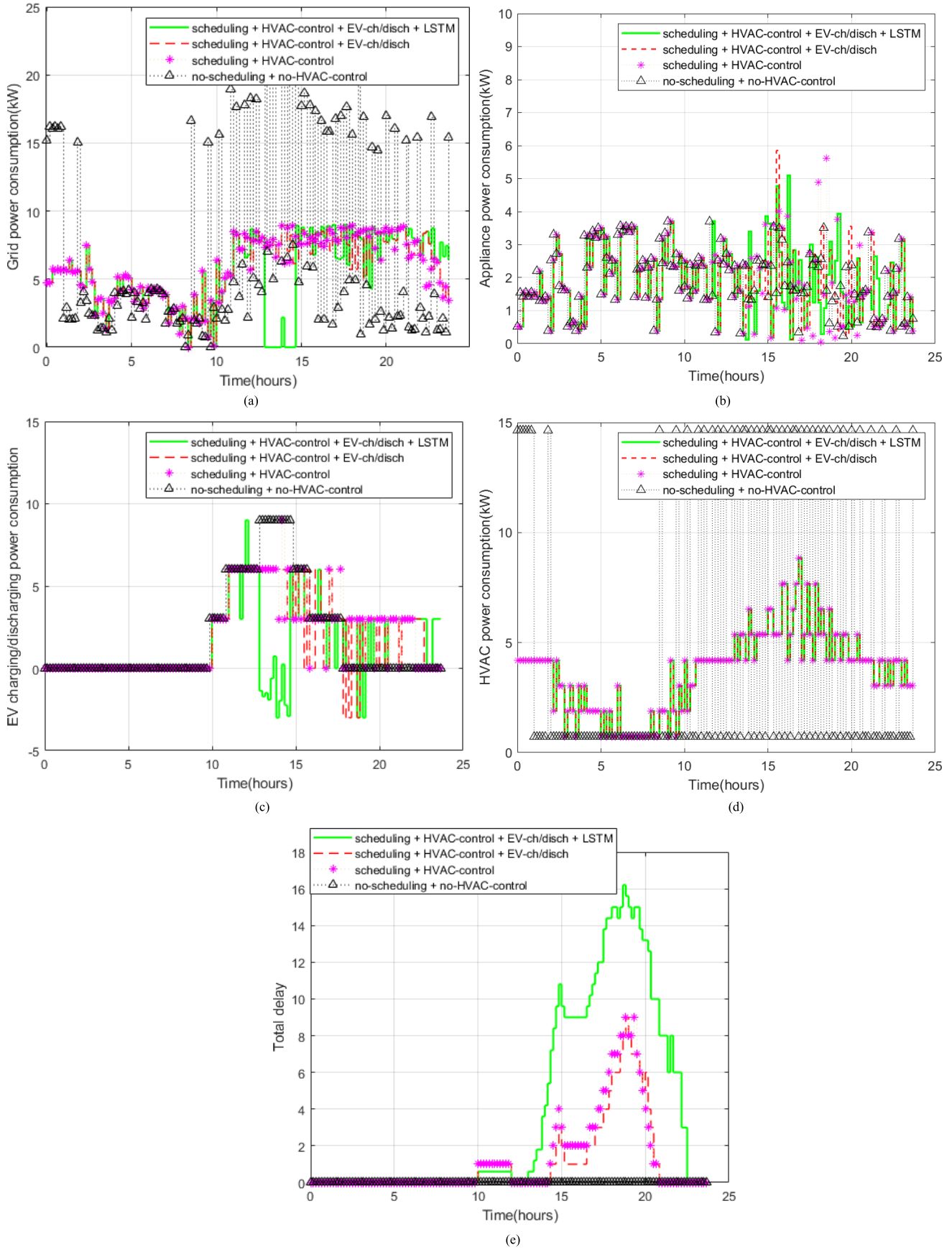

FIGURE 8. Operation of nanogrid consisting of 3 houses with PV power production 2kW/house: (a) grid power consumption; (b) power consumption of electric appliances other than 3 EVs and HVAC; (c) charging/discharging; (d) power consumption of HVAC; (e) total delay. Negative power consumption of EVs indicates discharging.

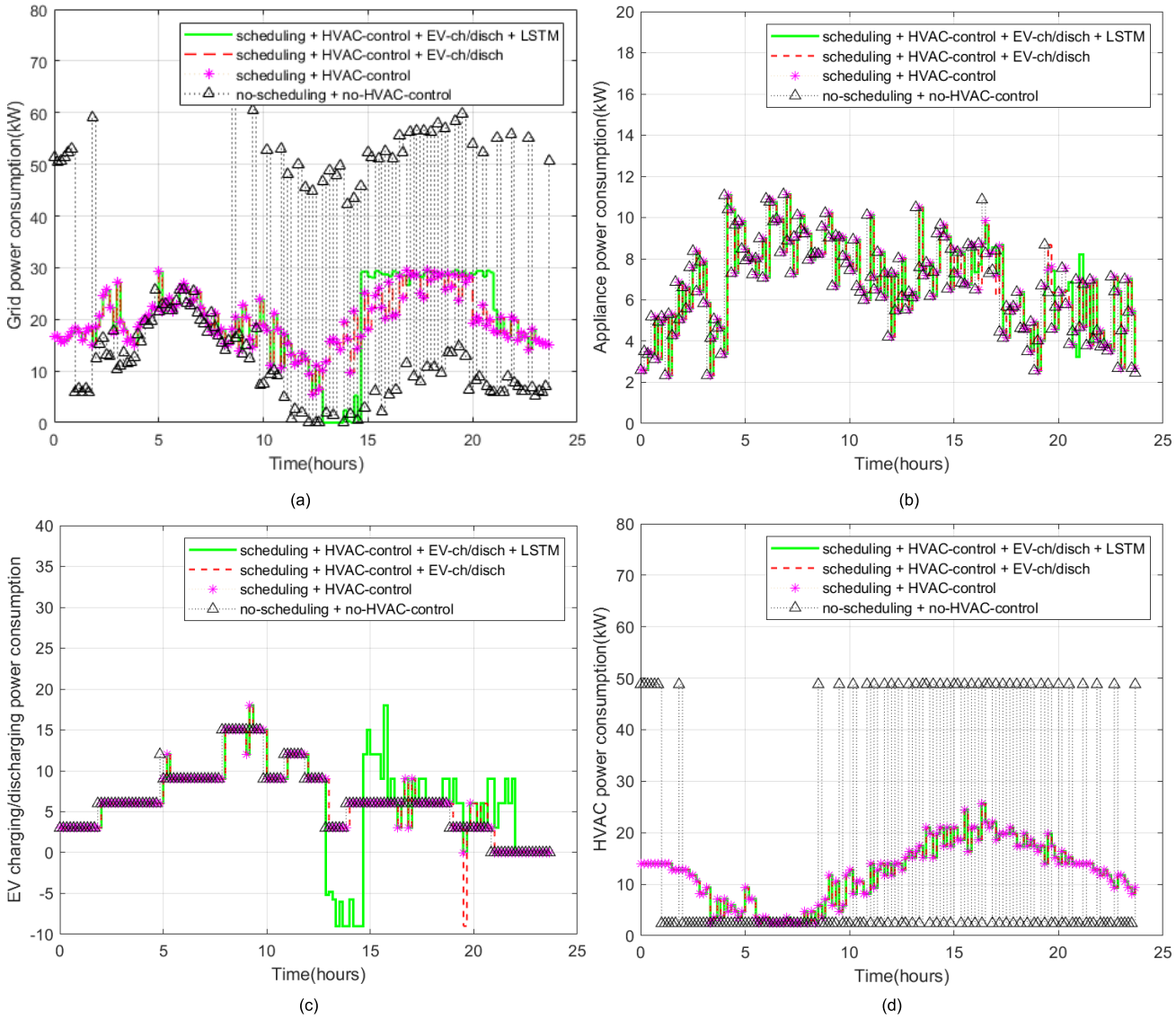

FIGURE 9. Operation of nanogrid consisting of 10 houses with PV power production 2kW/house: (a) grid power consumption; (b) power consumption of electric appliances other than 10 EVs and HVAC; (c) EV charging/discharging; (d) power consumption of HVAC. Negative power consumption of EVs indicates discharging.

the ''scheduling+HVAC-control+EV-ch/disch'' scheme the EVs are continually charged until 18hrs and discharged at 18hrs to reduce peak load. Most of the EV discharging by the ''scheduling+HVAC-control+EV-ch/disch+LSTM'' scheme occurs before 15hrs and another one at 18hrs. Beyond 18hrs, no more EV discharging is observed, due to the time constraint $d_{EV,\max}$ Due to EV charging after 15hrs, following EV discharging, in the ''scheduling+HVAC-control+EV-ch/disch+LSTM'' scheme, significant delay before full charging is created. On the other hand, EV discharging and charging appear alternately from 18hrs by the ''scheduling+HVAC-control+EV-ch/disch'' scheme. This alternate EV discharging and charging cause decreased total delay. Though charging rate of an EV is 3kW, discharging rate depending on instantaneous grid power consumption is not in the unit of 3kW. It is because the grid power consumption becomes 0 at that time even with discharging power less than 3kW. Due to the variation pattern of outdoor temperature in Fig.6, the operation of the ''no-scheduling+no-HVAC-control'' is relatively inactive over the range between 2hrs and 8hrs after intensive cooling by the air-conditioners in the early hours, as presented in Fig.8(d). Since the Markov chain model is common to all schemes considered for this simulation and HVAC is non-shiftable, variation of HVAC power consumption in the ''scheduling+HVAC-control'' scheme is identical with those of the ''scheduling+HVAC-control+EV-ch/disch'' scheme and ''scheduling+HVAC-control+EV-ch/disch+LSTM'' scheme. The reduction of power consumption of the HVAC by the control according to the resident location is clearly demonstrated in Fig.8(d). Like Fig.8(b-c), portion of power consumption in Fig.8(d) comes from PV power and the rest from the grid.

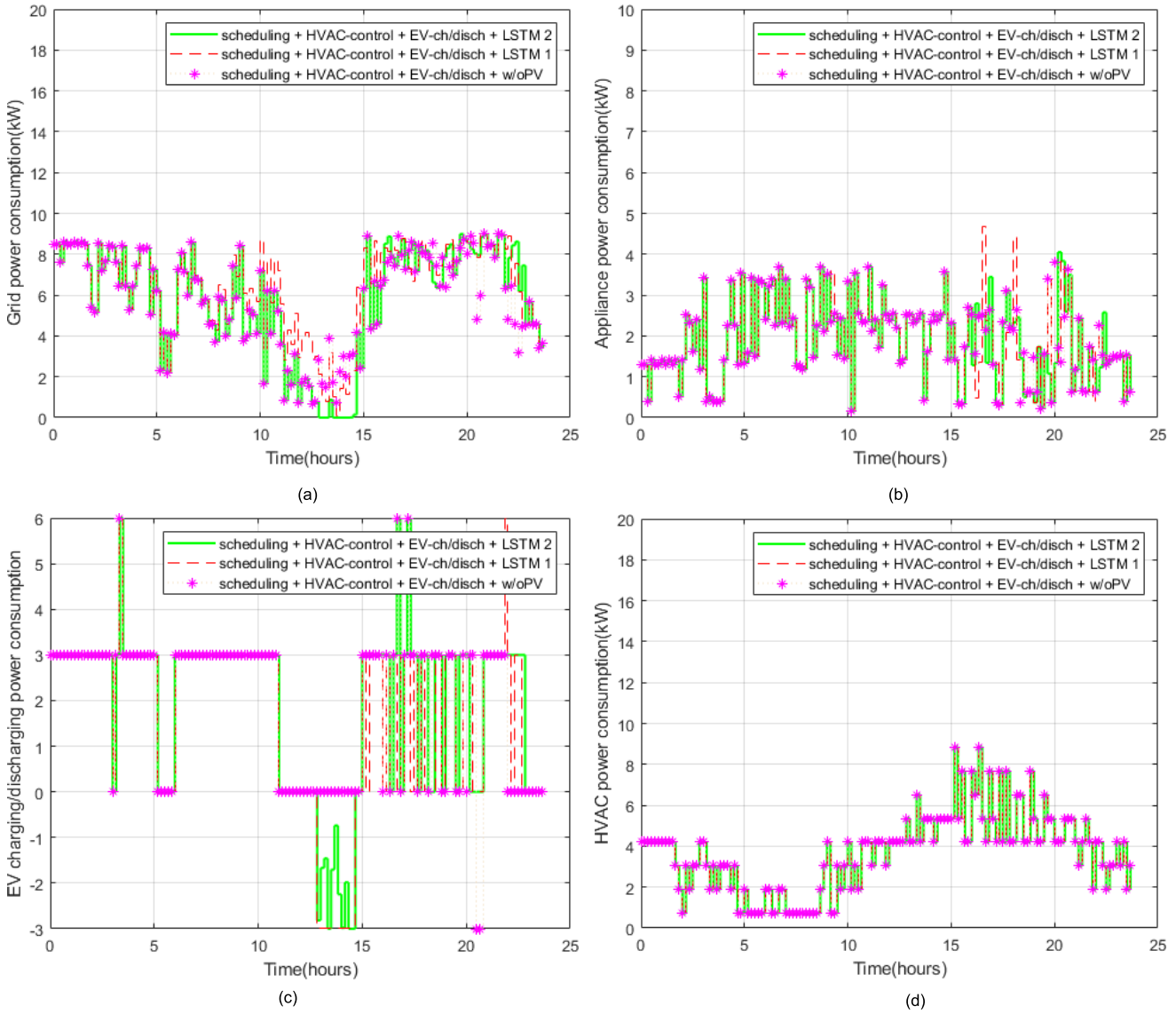

FIGURE 10. Operation of nanogrid consisting of 3 houses: (a) grid power consumption; (b) power consumption of electric appliances other than 3 EVs and HVAC; (c) EV charging/discharging; (d) power consumption of HVAC.

Variation of total delay of shiftable appliances, including EVs, is presented in Fig. 8 (e). Total delay is the objective function in (3a). In case of "no-scheduling+no-HVAC control" scheme, no delay occurs because there is no scheduling. Total delay of proposed scheme with LSTM network is the largest over 13-24hrs, due to significant EV discharging which requires full charging by 24hrs. Total delay of conventional "scheduling+HVAC-control+EV-ch/disch" scheme is less than that of proposed scheme over 13-24hrs, due to smaller amount of discharged energy according to emergency-based discharging condition in (5a). Total delay of "scheduling+HVAC-control" scheme that requires EV charging only is close to that of "scheduling+HVAC-control+EV-ch/disch" scheme, since discharged energy of EVs with "scheduling+HVAC-control+EV-ch/disch" scheme is not large. Total delay of shiftable appliances with the 3 schemes requiring scheduling is approaching maximum around 17hrs due to large power consumption of HVAC.

As seen in Fig.8(a), the "no-scheduling + no-HVAC-control" scheme often results in instantaneous grid power consumption $PW(n)$ well above the $PW^{\max}$ 9kW, whereas the other three schemes are able to keep the grid power consumption below $PW^{\max}$ throughout the day. Electricity costs of grid power consumption over 24hrs are \$12.32, \$13.53, \$13.62, \$17.59, when "scheduling + HVAC-control + EV-ch/disch + LSTM" scheme, "scheduling + HVAC-control + EV-ch/disch" scheme, "scheduling + HVAC-control" scheme, and "no-scheduling + no-HVAC-control" scheme are used, respectively.

Simulation #2: Effect of EV charging/discharging on the operation of nanogrid consisting of 10 houses with PV power production.

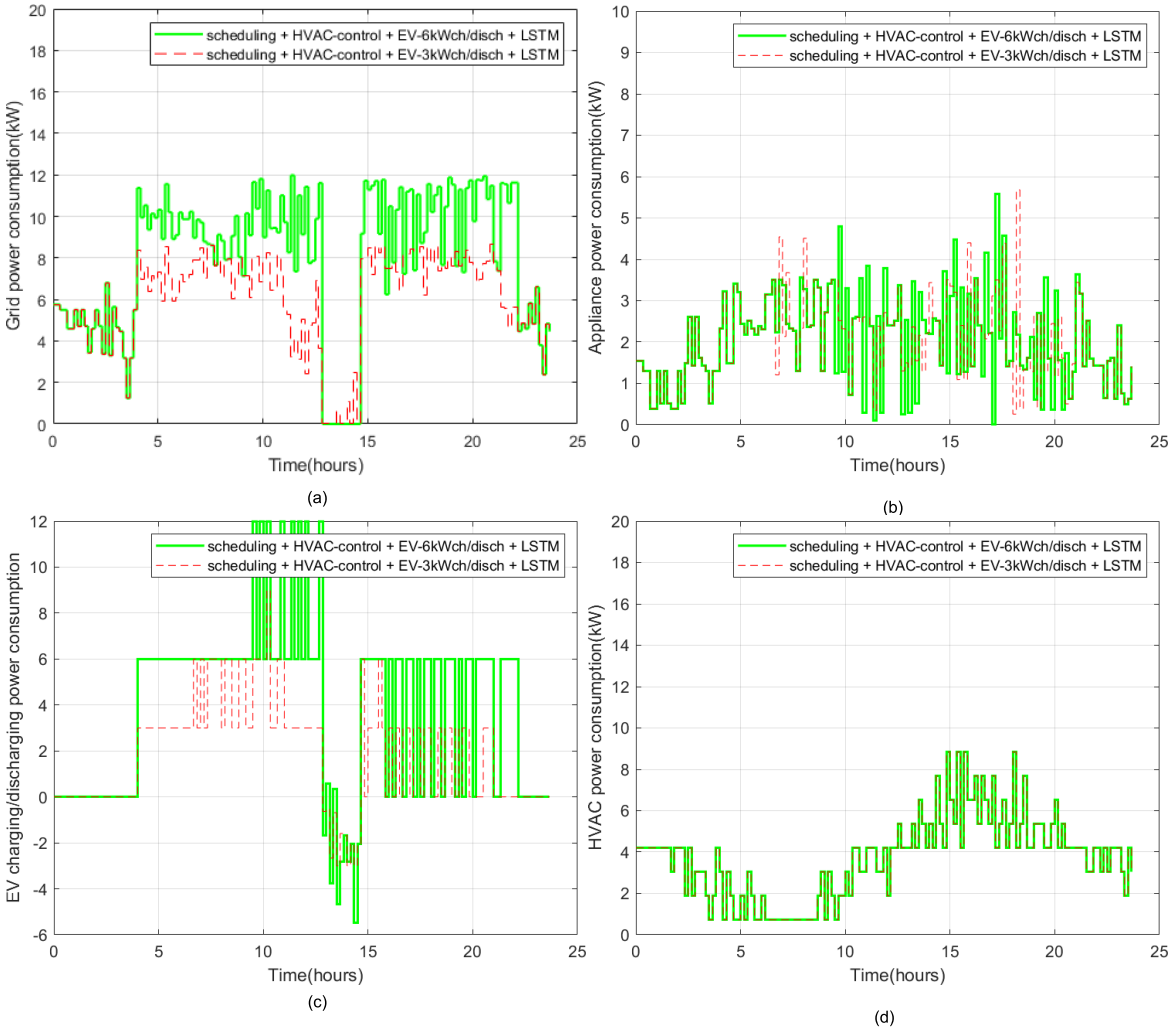

FIGURE 11. Operation of nanogrid consisting of 3 houses with PV power production 2kW/house when rates of EV charging are 3kW and 6kW: (a) grid power consumption; (b) power consumption of electric appliances other than 3 EVs and HVAC; (c) EV charging/discharging; (d) power consumption of HVAC.

Figure 9 presents the power consumption of 4 different power management schemes in the nanogrid consisting of 10 houses. The maximum PV power production of rooftop PV panels of each house is also 2kW. This simulation can emphasize the benefit, e.g., reduction of electricity cost, obtained from the proposed scheme based on the predicted PV power production. Figure 9(a) shows the grid power consumption $PW(n) - PW^{PV}(n)$. It is also seen in Fig.9(a) that EV charging according to "scheduling + HVAC-control + EV-ch/disch + LSTM" scheme occurs over the time zone before 13hrs, where most of the time zone corresponds to low rate of electricity, and EV discharging takes place around 15hrs, pertaining to high rate of electricity. Similar to Fig.8(b), the variation of power consumption of non-shiftable and shiftable appliances according to each scheme is close to each other. Similarly to simulation #1, operation of the HVAC depending on the resident location allows more power to be consumed by other electric appliances, which leads to more flexible power management with the EVs. It is seen in Fig.9(c) that the EVs are kept charged until 13hrs by the "scheduling + HVAC-control + EV-ch/disch + LSTM" scheme for discharging between 13-15hrs to save electricity cost. Figure 9(d) shows the power consumption of HVAC. Electricity costs of grid power consumption over 24hrs are \$53.92, \$57.96, \$57.99, \$70.59, when "scheduling + HVAC-control + EV-ch/disch + LSTM" scheme, "scheduling + HVAC-control + EV-ch/disch" scheme, "scheduling + HVAC-control" scheme, and "no-scheduling + no-HVAC-control" scheme are used, respectively.

Simulation #3: Effect of different level of PV power production on the operation of nanogrid consisting of 3 houses.

Figure 10 shows the results of power management according to different level of PV power production. The "scheduling + HVAC-control + EV-ch/disch + LSTM2" and "scheduling + HVAC-control + EV-ch/disch + LSTM1" represent power management scheme "scheduling + HVAC-control + EV-ch/disch + LSTM" with PV power production 2kW/house, 1kW/house, respectively. The "scheduling + HVAC-control + EV-ch/disch + w/oPV" scheme represents the "scheduling + HVAC-control + EV-ch/disch" scheme

without PV production of houses. As shown in Fig.10(a), the "scheduling + HVAC-control + EV-ch/disch + LSTM2" scheme leads to the lowest power consumption in general among the three schemes due to the increased PV power production. The trends of power consumption of EVs, HVAC, and other electric appliances are almost the same as shown in Fig.10(b-d). Figure 10(c) shows that initiation of charging the first EV occurs at 0hr, the second EV at 6hrs, and the third at 15hrs. EV discharging during 13-15hrs in Fig.10(c) by "scheduling + HVAC-control + EV-ch/disch + LSTM2" scheme can make $PW(n) - PW^{PV}(n)$ in Fig.10(a) 0 with discharged power less than 3kW, due to sufficient PV power, while the $PW(n) - PW^{PV}(n)$ in Fig.10(a) with "scheduling + HVAC-control + EV-ch/disch + LSTM1" cannot be 0 even with 3kW discharged power. The "scheduling + HVAC-control + EV-ch/disch" scheme causes EV discharging over short period of time after 20hrs, which is matched with the decreased grid power consumption in Fig.10(a) observed after 20hrs. Electricity costs for 24hrs are \$10.3262, \$11.8360, \$17.1448, when "scheduling + HVAC-control + EV-ch/disch + LSTM2" scheme, "scheduling + HVAC-control + EV-ch/disch + LSTM1" scheme, "scheduling + HVAC-control + EV-ch/disch + w/oPV" scheme, are used, respectively.

Simulation #4: Effect of different rate of EV charging on the operation of nanogrid consisting of 3 houses with PV power production.

Two types of EVs are considered in this simulation. The first type of EVs has battery capacity requiring 2.5kWh for a 10% increment of SOC and the second type of EVs demands 5kWh for a 10% increment of SOC. For different types of EVs, different charging rates 3kW and 6kW are considered. Figure 11 presents the power consumption when the rates of EV charging are 3kW and 6kW. For the "scheduling+HVAC-control+EV-**6kWch/disch**+LSTM" scheme, rate of EV charging is set to 6 kW and $PW^{\max}$ is 12kW, while in case of "scheduling+HVAC-control+EV-**3kWch/disch**+LSTM" scheme, the rate of EV charging is set to 3 kW and the $PW^{\max}$ is 9kW. As shown in Fig.11(a), the "scheduling+HVAC-control+EV-**6kWch/disch**+LSTM" scheme makes the grid power consumption $PW(n) - PW^{PV}(n)$ close to the $PW^{\max}$ 12kW from 15hrs, corresponding to high electricity cost. EV discharging over the time zone between 13hrs and 15hrs makes the grid power consumption 0, as seen in Fig.11(a). Figure 11(b) shows identical pattern of power consumption of non-shiftable and shiftable appliances until 7hrs. Power consumption of shiftable appliances in the "scheduling+HVAC-control+EV-**6kWch/disch**+LSTM" scheme is more delayed in general due to double rate of EV charging that leaves less room for power consumption of shiftable appliances. In Fig.11(c), EV charging is also continued until 13hr for discharging between 13hr and 15hr. Although the rate of EV charging is changed, there is no basic difference between the two schemes in power consumption of non-shiftable HVAC, as seen in Fig.11(d). Due to double rate charging between 9hrs and 13hrs and similar level of discharging from 13hrs to 15hrs, the "scheduling+HVAC-control+EV-**6kWch/disch**+LSTM" scheme is not more advantageous than the "scheduling+HVAC-control+EV-**3kWch/disch**+LSTM" scheme. Electricity costs for 24hrs are \$17.8071 with "scheduling+HVAC-control+EV-**6kWch/disch**+LSTM" scheme and \$13.4461 with "scheduling+HVAC-control+EV-**3kWch/disch**+LSTM" scheme.

TABLE 4. Comparison of electricity cost according to power management scheme.

Scheme	Simulation index (Color of plot)	Electricity cost ($)
no-scheduling+no-HVAC-control	#1 (Black)	\$17.5941
	#2 (Black)	\$70.5975
scheduling+HVAC-control	#1 (Magenta)	\$13.6203
	#2(Magenta)	\$57.9993
scheduling+HVAC-control+EV-ch/disch	#1(Red)	\$13.5310
	#2(Red)	\$57.9640
scheduling+HVAC-control+EV-ch/disch+w/oPV	#3(Magenta)	\$17.1448
scheduling+HVAC-control+EV-ch/disch+LSTM	#1(Green)	\$12.3219
	#2(Green)	\$53.9286
scheduling+HVAC-control+EV-ch/disch+LSTM2	#3(Green)	\$10.3262
scheduling+HVAC-control+EV-ch/disch+LSTM1	#3(Red)	\$11.8360
scheduling+HVAC-control+EV-**6kWch/disch**+LSTM	#4(Green)	\$17.8071
scheduling+HVAC-control+EV-**3kWch/disch**+LSTM	#4(Red)	\$13.4461

TABLE 4 lists up electricity cost according to the power management scheme. As seen in the table, the power management involving EV discharging according to predicted power management results in the lowest electricity cost among the considered schemes. The reduction of electricity cost by the efficient EV charging/discharging enabled by the LSTM network is roughly 7%.

V. CONCLUSION

Predictive power management is considered in this paper to reduce the electricity cost of nanogrid characterized by V2G configuration and PV power production. In the proposed scheme, the LSTM network is used to predict PV power

production. According to the predicted PV power production, EV mode is determined. EVs considered in this work act like ESSs when they are discharged. If the predicted PV power production as well as outdoor temperature in relation to indoor temperature corresponds to the condition on EV discharging, the EV can discharge to reduce the electricity cost. It is shown that the EV discharging in predictive power management occurs when the rate of electricity is high and thus reduces electricity cost in the presence of PV power. Since time intervals for EV charging are distinct from those for EV discharging, EV charging is also affected by the predicted PV power production. Considering the power scale of EV charging/discharging relative to other electric appliances, efficient EV charging/discharging is critically important for nanogrid power management. From this viewpoint, the proposed power management scheme for nanogrid is expected to be useful for the reduction of electricity cost. In simulations, the proposed power management scheme is compared in terms of electricity cost with other power management schemes. The results of simulations show that the predictive power management scheme achieves a significant reduction of electricity cost. Particularly, it achieves a 5%∼7% reduction of electricity cost as compared to other power management schemes, which do not involve prediction of PV power production.

REFERENCES

[1] X. Wu, X. Hu, Y. Teng, S. Qian, and R. Cheng, "Optimal integration of a hybrid solar-battery power source into smart home nanogrid with plug-in electric vehicle," *J. Power Sources*, vol. 363, pp. 277–283, Sep. 2017.

[2] D. Burmester, R. Rayudu, W. Seah, and D. Akinyele, "A review of nanogrid topologies and technologies," *Renew. Sustain. Energy Rev.*, vol. 67, pp. 760–775, Jan. 2017.

[3] A. Werth, N. Kitamura, and K. Tanaka, "Conceptual study for open energy systems: Distributed energy network using interconnected DC nanogrids," *IEEE Trans. Smart Grid*, vol. 6, no. 4, pp. 1621–1630, Jul. 2015.

[4] S. Parhizi, H. Lotfi, A. Khodaei, and S. Bahramirad, "State of the art in research on microgrids: A review," *IEEE Access*, vol. 3, pp. 890–925, 2015.

[5] M. Nasir, Z. Jin, H. A. Khan, N. A. Zaffar, J. C. Vasquez, and J. M. Guerrero, "A decentralized control architecture applied to DC nanogrid clusters for rural electrification in developing regions," *IEEE Trans. Power Electron.*, vol. 34, no. 2, pp. 1773–1785, Feb. 2019.

[6] R. Adda, O. Ray, S. K. Mishra, and A. Joshi, "Synchronous-reference-frame-based control of switched boost inverter for standalone DC nanogrid applications," *IEEE Trans. Power Electron.*, vol. 28, no. 3, pp. 1219–1233, Mar. 2013.

[7] M. Marzband, H. Alavi, S. S. Ghazimirsaeid, H. Uppal, and T. Fernando, "Optimal energy management system based on stochastic approach for a home microgrid with integrated responsive load demand and energy storage," *Sustain. Cities Soc.*, vol. 28, pp. 256–264, Jan. 2017.

[8] C. D. Korkas, S. Baldi, I. Michailidis, and E. B. Kosmatopoulos, "Occupancy-based demand response and thermal comfort optimization in microgrids with renewable energy sources and energy storage," *Appl. Energy*, vol. 163, pp. 93–104, Feb. 2016.

[9] S. Lee, J. Lee, H. Jung, J. Cho, J. Hong, S. Lee, and D. Har, "Optimal power management for nanogrids based on technical information of electric appliances," *Energy Buildings*, vol. 191, pp. 174–186, May 2019.

[10] K. P. Exchange, "Survey report of home appliance supply rate and electricity consumption behavior of residential customers," Korea Power Exchange, Naju-si, South Korea, Tech. Rep., 2006.

[11] J. Widén and E. Wäckelgård, "A high-resolution stochastic model of domestic activity patterns and electricity demand," *Appl. Energy*, vol. 87, no. 6, pp. 1880–1892, Jun. 2010.

[12] J. Virote and R. Neves-Silva, "Stochastic models for building energy prediction based on occupant behavior assessment," *Energy Buildings*, vol. 53, pp. 183–193, Oct. 2012.

[13] R. C. Green, L. Wang, and M. Alam, "The impact of plug-in hybrid electric vehicles on distribution networks: A review and outlook," in *Proc. IEEE PES Gen. Meeting*, Jul. 2010, pp. 1–8.

[14] A. K. Srivastava, B. Annabathina, and S. Kamalasadan, "The challenges and policy options for integrating plug-in hybrid electric vehicle into the electric grid," *Electr. J.*, vol. 23, no. 3, pp. 83–91, Apr. 2010.

[15] X. Yu, "Impacts assessment of PHEV charge profiles on generation expansion using national energy modeling system," in *Proc. IEEE Power Energy Soc. Gen. Meeting*, vols. 1–2, Jul. 2008, pp. 4857–4861.

[16] P. Denholm and W. Short, "An evaluation of utility system impacts and benefits of optimally dispatched plug-in hybrid electric vehicles," Nat. Renew. Energy Lab., Golden, CO, USA, Tech. Rep. NREL/TP-620-40293, 2006.

[17] C. Silvestre, D. M. Sousa, and A. Roque, "Reactive power compensation using on board stored energy in electric vehicles," in *Proc. 38th Annu. Conf. IEEE Ind. Electron. Soc. (IECON)*, Oct. 2012, pp. 5227–5232.

[18] M. A. Fasugba and P. T. Krein, "Cost benefits and vehicle-to-grid regulation services of unidirectional charging of electric vehicles," in *Proc. IEEE Energy Convers. Congr. Expo.*, Sep. 2011, pp. 827–834.

[19] B. Tarroja, J. D. Eichman, L. Zhang, T. M. Brown, and S. Samuelsen, "The effectiveness of plug-in hybrid electric vehicles and renewable power in support of holistic environmental goals: Part 1—Evaluation of aggregate energy and greenhouse gas performance," *J. Power Sources*, vol. 257, pp. 461–470, Jul. 2014.

[20] B. Tarroja, J. D. Eichman, L. Zhang, T. M. Brown, and S. Samuelsen, "The effectiveness of plug-in hybrid electric vehicles and renewable power in support of holistic environmental goals: Part 2—Design and operation implications for load-balancing resources on the electric grid," *J. Power Sources*, vol. 278, pp. 782–793, Mar. 2015.

[21] C. Liu, K. T. Chau, D. Wu, and S. Gao, "Opportunities and challenges of vehicle-to-home, vehicle-to-vehicle, and vehicle-to-grid technologies," *Proc. IEEE*, vol. 101, no. 11, pp. 2409–2427, Nov. 2013.

[22] K. An, K.-B. Song, and K. Hur, "Incorporating charging/discharging strategy of electric vehicles into security-constrained optimal power flow to support high renewable penetration," *Energies*, vol. 10, no. 5, p. 729, May 2017.

[23] Y. Wang and D. Infield, "Markov chain Monte Carlo simulation of electric vehicle use for network integration studies," *Int. J. Electr. Power Energy Syst.*, vol. 99, pp. 85–94, Jul. 2018.

[24] J. Rolink and C. Rehtanz, "Large-scale modeling of grid-connected electric vehicles," *IEEE Trans. Power Del.*, vol. 28, no. 2, pp. 894–902, Apr. 2013.

[25] A. Ul-Haq, C. Cecati, and E. El-Saadany, "Probabilistic modeling of electric vehicle charging pattern in a residential distribution network," *Electr. Power Syst. Res.*, vol. 157, pp. 126–133, Apr. 2018.

[26] Y. Cao, S. Tang, C. Li, P. Zhang, Y. Tan, Z. Zhang, and J. Li, "An optimized EV charging model considering TOU price and SOC curve," *IEEE Trans. Smart Grid*, vol. 3, no. 1, pp. 388–393, Mar. 2012.

[27] Y. He, B. Venkatesh, and L. Guan, "Optimal scheduling for charging and discharging of electric vehicles," *IEEE Trans. Smart Grid*, vol. 3, no. 3, pp. 1095–1105, Sep. 2012.

[28] Y.-M. Wi, J.-U. Lee, and S.-K. Joo, "Electric vehicle charging method for smart homes/buildings with a photovoltaic system," *IEEE Trans. Consum. Electron.*, vol. 59, no. 2, pp. 323–328, May 2013.

[29] S. Lee, S. Myung, J. Hong, and D. Har, "Reverse osmosis desalination process optimized for maximum permeate production with renewable energy," *Desalination*, vol. 398, pp. 133–143, Nov. 2016.

[30] S. Lee, J. Hong, and D. Har, "Jointly optimized control for reverse osmosis desalination process with different types of energy resource," *Energy*, vol. 117, pp. 116–130, Dec. 2016.

[31] S. Lee, H.-Y. Cho, and D. Har, "Operation optimization with jointly controlled modules powered by hybrid energy source: A case study of desalination," *Renew. Sustain. Energy Rev.*, vol. 81, pp. 3070–3080, Jan. 2018.

[32] M. Sechilariu, B. Wang, and F. Locment, "Building integrated photovoltaic system with energy storage and smart grid communication," *IEEE Trans. Ind. Electron.*, vol. 60, no. 4, pp. 1607–1618, Apr. 2013.

[33] F. Marra, G. Y. Yang, C. Traeholt, E. Larsen, J. Ostergaard, B. Blazic, and W. Deprez, "EV charging facilities and their application in LV feeders with photovoltaics," *IEEE Trans. Smart Grid*, vol. 4, no. 3, pp. 1533–1540, Sep. 2013.

[34] S. Srivastava and S. Lessmann, "A comparative study of LSTM neural networks in forecasting day-ahead global horizontal irradiance with satellite data," *Sol. Energy*, vol. 162, pp. 232–247, Mar. 2018.

[35] S. Lee, S. Kim, M. Seo, and D. Har, "Synchronization of frequency hopping by LSTM network for satellite communication system," *IEEE Commun. Lett.*, vol. 23, no. 11, pp. 2054–2058, Nov. 2019.

[36] S. Lee, L. F. Vecchietti, H. Jin, J. Hong, and D. Har, "Power management by LSTM network for nanogrids," *IEEE Access*, vol. 8, pp. 24081–24097, 2020.

[37] M. B. Arias and S. Bae, "Electric vehicle charging demand forecasting model based on big data technologies," *Appl. Energy*, vol. 183, pp. 327–339, Dec. 2016.

[38] *Benefits of Demand Response in Electricity Markets and Recommendations for Achieving Them. A Report to The United States Congress Pursuant to Section 1252 of the Energy Policy Act of 2005*, Dept. Energy, Washington, DC, USA, 2006.

[39] S. Deilami, A. S. Masoum, P. S. Moses, and M. A. S. Masoum, "Real-time coordination of plug-in electric vehicle charging in smart grids to minimize power losses and improve voltage profile," *IEEE Trans. Smart Grid*, vol. 2, no. 3, pp. 456–467, Sep. 2011.

[40] R. J. Bessa and M. A. Matos, "Optimization models for EV aggregator participation in a manual reserve market," *IEEE Trans. Power Syst.*, vol. 28, no. 3, pp. 3085–3095, Aug. 2013.

[41] L. Gan, U. Topcu, and S. H. Low, "Optimal decentralized protocol for electric vehicle charging," *IEEE Trans. Power Syst.*, vol. 28, no. 2, pp. 940–951, May 2013.

[42] O. Erdinc, N. G. Paterakis, T. D. P. Mendes, A. G. Bakirtzis, and J. P. S. Catalao, "Smart household operation considering bi-directional EV and ESS utilization by real-time pricing-based DR," *IEEE Trans. Smart Grid*, vol. 6, no. 3, pp. 1281–1291, May 2015.

[43] M. Honarmand, A. Zakariazadeh, and S. Jadid, "Optimal scheduling of electric vehicles in an intelligent parking lot considering vehicle-to-grid concept and battery condition," *Energy*, vol. 65, pp. 572–579, Feb. 2014.

[44] T. Ray and P. Saini, "Engineering design optimization using a swarm with an intelligent information sharing among individuals," *Eng. Optim.*, vol. 33, no. 6, pp. 735–748, Aug. 2001.

[45] J. A. Vasconcelos, J. A. Ramirez, R. H. C. Takahashi, and R. R. Saldanha, "Improvements in genetic algorithms," *IEEE Trans. Magn.*, vol. 37, no. 5, pp. 3414–3417, Sep. 2001.

[46] A. E. Eiben, R. Hinterding, and Z. Michalewicz, "Parameter control in evolutionary algorithms," *IEEE Trans. Evol. Comput.*, vol. 3, no. 2, pp. 124–141, Jul. 1999.

[47] K. M. Tan, V. K. Ramachandaramurthy, and J. Y. Yong, "Integration of electric vehicles in smart grid: A review on vehicle yo grid technologies and optimization techniques," *Renew. Sustain. Energy Rev.*, vol. 53, pp. 720–732, Jan. 2016.

[48] R. Yang and L. Wang, "Multi-objective optimization for decision-making of energy and comfort management in building automation and control," *Sustain. Cities Soc.*, vol. 2, no. 1, pp. 1–7, Feb. 2012.

[49] D. Kolokotsa, A. Pouliezos, G. Stavrakakis, and C. Lazos, "Predictive control techniques for energy and indoor environmental quality management in buildings," *Building Environ.*, vol. 44, no. 9, pp. 1850–1863, Sep. 2009.

[50] V. Sharma, U. Cali, V. Hagenmeyer, R. Mikut, and J. Á. G. Ordiano, "Numerical weather prediction data free solar power forecasting with neural networks," in *Proc. 9th Int. Conf. Future Energy Syst.*, Jun. 2018, pp. 604–609.

[51] F. Barbieri, S. Rajakaruna, and A. Ghosh, "Very short-term photovoltaic power forecasting with cloud modeling: A review," *Renew. Sustain. Energy Rev.*, vol. 75, pp. 242–263, Aug. 2017.

[52] H. Shi, M. Xu, and R. Li, "Deep learning for household load forecasting—A novel pooling deep RNN," *IEEE Trans. Smart Grid*, vol. 9, no. 5, pp. 5271–5280, Sep. 2018.

[53] S. Hochreiter and J. Schmidhuber, "Long short-term memory," *Neural Comput.*, vol. 9, no. 8, pp. 1735–1780, Nov. 1997.

[54] C. Lin, S. Xu, Z. Li, B. Li, G. Chang, and J. Liu, "Thermal analysis of large-capacity LiFePO4 power batteries for electric vehicles," *J. Power Sources*, vol. 294, pp. 633–642, Oct. 2015.

[55] M. S. H. Lipu, M. A. Hannan, A. Hussain, M. M. Hoque, P. J. Ker, M. H. M. Saad, and A. Ayob, "A review of state of health and remaining useful life estimation methods for lithium-ion battery in electric vehicles: Challenges and recommendations," *J. Cleaner Prod.*, vol. 205, pp. 115–133, Dec. 2018.

[56] D. P. Kingma and J. Ba, "Adam: A method for stochastic optimization," 2014, *arXiv:1412.6980*. [Online]. Available: http://arxiv.org/abs/1412.6980

[57] W. Kirchgässner, O. Wallscheid, and J. Bocker, "Deep residual convolutional and recurrent neural networks for temperature estimation in permanent magnet synchronous motors," in *Proc. IEEE Int. Electr. Mach. Drives Conf. (IEMDC)*, May 2019, pp. 1439–1446.

SANGKEUM LEE received the B.S. degree in electronics and information engineering from Korea University, in 2016, and the M.S. degree from KAIST, where he is currently pursuing the Ph.D. degree. He is also a member of the Vehicular Intelligence Laboratory, The Cho Chun Shik Graduate School for Green Transportation, KAIST. His main research interest include the areas of sensor network systems and its supporting technologies, such as optimization, neural network, sensor networks, and power systems.

HOJUN JIN received the B.S. degree in mechanical engineering from the Korea University of Technology and Education, South Korea, in 2018, and the M.S. degree from The Cho Chun Shik Graduate School of Green Transportation, Korea Advanced Institute of Science and Technology, South Korea, where he is currently pursuing the Ph.D. degree. His main research interest include the areas of optimization, scheduling, artificial intelligence, and power systems.

LUIZ FELIPE VECCHIETTI received the B.Sc. degree in electronics and computer engineering and the M.Sc. degree from the Federal University of Rio de Janeiro, in 2015 and 2017, respectively. He is currently pursuing the Ph.D. degree with The Cho Chun Shik Graduate School of Green Transportation, KAIST. His research interests include machine learning, digital signal processing, and applied deep learning.

JUNHEE HONG (Member, IEEE) received the B.S., M.S., and Ph.D. degrees in electrical engineering from Seoul National University, Seoul, South Korea, in 1987, 1989, and 1995, respectively. Since 1995, he has been a Professor with the Department of Energy IT, Gachon University, Kyunggi-do, South Korea. His research interests include smart grid, supergrid, renewable energy, digitalization of electric power, and energy policy.

DONGSOO HAR (Senior Member, IEEE) received the B.Sc. and M.Sc. degrees in electronics engineering from Seoul National University, and the Ph.D. degree in electrical engineering from Polytechnic University, Brooklyn, NY, USA. He is currently a faculty member of KAIST. He was a recipient of the Best Paper Award (Jack Neubauer Award) from the IEEE Transactions on Vehicular Technology, in 2000. He is an Associate Editor of the IEEE Sensors Journal. He authored and published more than 100 articles in international journals and conferences. He was the member of advisory board, a Program Chair, a Vice Chair, and a General Chair of international conferences. He also presented invited talks and keynote in international conferences. His main research interests include optimization of communication system operation and transportation system development with embedded artificial intelligence.